RSC Advances

PAPER

View Article Online
View Journal | View Issue

Cite this: *RSC Adv.*, 2020, **10**, 22397

Proline derived guanidine catalysts forge extensive H-bonded architectures: a solution and solid state study†

Zahraa S. Al-Taie,[ab] Simon R. Anetts,[b] Jeppe Christensen,[cd] Simon J. Coles,[d] Peter N. Horton,[d] Daniel M. Evans,[b] Leigh F. Jones,[e] Frank F. J. de Kleijne,[b] Shaun M. Ledbetter,[b] Yassin T. H. Mehdar,[b] Patrick J. Murphy *[b] and Jack A. Wilson[b]

Received 17th September 2019
Accepted 25th February 2020

DOI: 10.1039/c9ra07508a

rsc.li/rsc-advances

The preparation of a range of amino acid derived guanidine organocatalysts is reported together with their application to the Michael addition of 2-hydroxy-1,4-napthoquinone to β-nitrostyrene, achieving a maximum ee of 56%. Some insight into the mechanism was sought by using X-ray crystallography and a detailed study of the intra- and intermolecular hydrogen bonding is reported.

Introduction

We recently reported[1] the Michael addition of 2-hydroxy-1,4-napthoquinone **1** to β-nitrostyrene **2** catalyzed by the tetracyclic guanidinium salts **3** in combination with L-proline **4**. It was observed that the two substrates which were unreactive on combination in THF were slowly converted to the product **5** with a $T_{1/2}$ of 465 h. The reaction was also catalyzed slowly in the presence of L-proline **4** with a $T_{1/2}$ of 579 h in THF. However if the two catalysts **3** and L-proline were used in combination the reaction proceeded with a $T_{1/2}$ of 80 h. Unfortunately no appreciable enantioselectivity was observed in any of the catalysed reactions which might be attributed to the site of reaction being too far removed from the point of asymmetric induction within the proposed intermediate **6** (Scheme 1).

The catalysis of the process by the guanidinium salt **3** in conjunction with L-proline **4** was of interest, as proline and proline derivatives have a long history of use in organocatalysis.[2] It is also known that several guanidine and guanidinium derivatives have proved effective as organocatalysts. We have reported the use of **3** and related in phase transfer alkylations and epoxidations with high ee's and its free base as a catalyst for Michael additions albeit in low ee.[3] Similarly Yu *et al.*[4] reported that guanidine **7** was an efficient catalyst for the Michael reaction of β-ketoesters to 2-nitrostyrene **2** with ee's of up to 95%. Terada *et al.* reported a series of novel axially chiral guanidines **8** as highly efficient Brønsted base catalysts to promote Michael reactions in high ee's.[5] Similarly, Najera *et al.* reported the benzimidazole catalyst **9** gave enantioselectivities in the Michael additions of malonates to nitrostyrene **2** with selectivity of up to 96% ee, in the presence of TFA as a co-catalyst.[6] These authors also reported the use of the 2-aminobenzimidazole-derived organocatalyst **10** for the efficient room temperature asymmetric conjugate addition of 1,3-diketones, β-ketoesters, and malonates to maleimides in up to 97% ee.[7] An interesting catalyst containing both guanidine and thiourea moieties **11** was reported by Shubina *et al.*[8] who reported the Michael additions of acetylacetone to β-nitrostyrene **2** in a low 25% ee. They reported that this poor selectivity was thought to arise from a high conformational activity of the guanidine–thiourea complex formed with the enolised acetylacetone, leading to several different transition states which are all of very similar energy (Fig. 1).[8]

We were interested in preparing a series of guanidines in an attempt to improve and extending the range of guanidines in organocatalysis. We initially decided to focus on the preparation of *N*-alkylated proline derived catalysts and were inspired

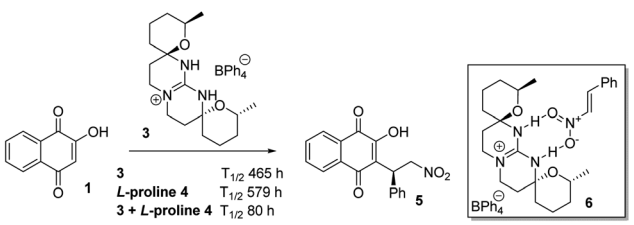

Scheme 1 Condition (a) β-nitrostyrene **2**, **3** (0.05 equiv.), L-proline **4** (0.05 equiv.), CH_2Cl_2, rt, 6 days 85%.

[a]Department of Chemistry, College of Science, Al-Nahrain University, Baghdad, Iraq
[b]School of Natural Sciences (Chemistry), Bangor University, Bangor, Gwynedd, LL57 2UW, UK. E-mail: paddy@bangor.ac.uk; Tel: +44 (0)1248 382392
[c]Diamond Light Source, Didcot, OX12 0DE, UK
[d]EPSRC National Crystallography Service, School of Chemistry, University of Southampton, Highfield, Southampton, SO17 1BJ, UK
[e]School of Biological, Physical and Forensic Sciences, University of Wolverhampton, WV1 1LY, UK

† Electronic supplementary information (ESI) available. CCDC 1952629–1952649. For ESI and crystallographic data in CIF or other electronic format see DOI: 10.1039/c9ra07508a

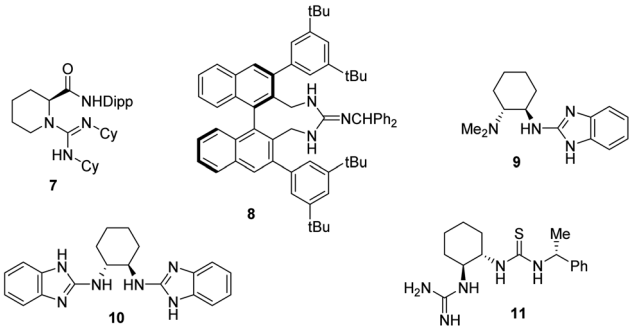

Fig. 1 Guanidine organocatalysts. Dipp = 2,6-diisopropylphenyl.

by the work of Altenbach *et al.* who reported[9] that the benzimidazole-proline derivative **12** was an effective catalyst in the Hajose–Parrishe–Edere–Sauere–Wiechert aldol reaction of 1,3-ketone **13**, leading to **14** in high yields and ee. Similarly, a report by Bhowmick *et al.* detailed[10] the structurally very simple hydrazine derivative of L-proline **15** which was a viable organocatalyst for the aldol reaction of ketones **16** with aldehydes **17**, leading to the aldol products **18** in 32–99% ee. Similalrly the low molecular weight cyclohexanediamine derived thiourea catalyst **19**, prepared[11] by Dixon *et al.*, was employed in intramolecular Michael additions of α,β-unsaturated esters. For example they reported the transformation of **20** into **21** in 86% yield and 94% ee using **19** as the catalyst (Scheme 2).

We envisaged the preparation of a range of guanidines **22**, based on a proline scaffold, which are both N-substituted and covalently bonded to a guanidine moiety *via* an amide bond. This concept was to allow ease of flexibility at these two sites and we hoped the catalysts might be "tunable" by modifying the proline nitrogen to influence steric interactions. Similarly, modification of the groups on the guanidine could also offer

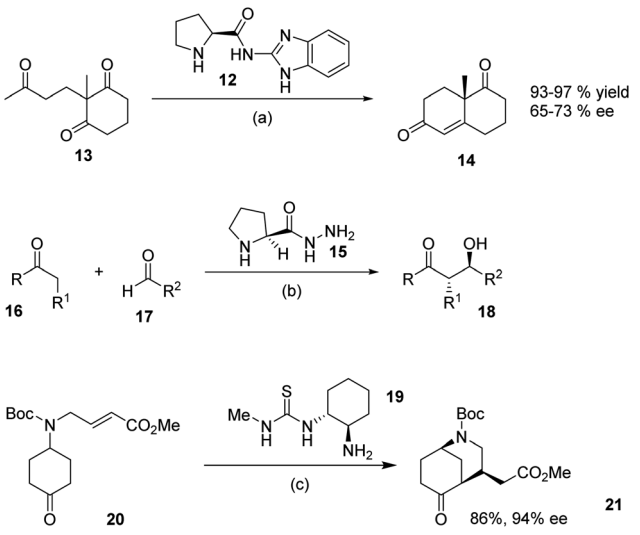

Scheme 2 Recent organocatalytic reactions. Conditions: (a) **12** (0.05 mmol), TFA (0.05 mmol), THF, DMSO, MeOH or H_2O, rt. 24 h. (b) **15** (0.1 equiv.), PTSA, (0.05 equiv.) in H_2O; R = alkyl, R^1 = H, alkyl, R^2 = aryl. (c) **19** (0.05 equiv.), $PhCO_2H$ (0.025 equiv.), CH_2Cl_2, 50 °C, 48 h.

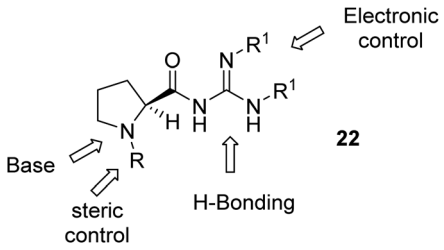

Fig. 2 Generic catalyst structure **22**. R = alkyl, R^1 = alkyl, aryl, acyl.

some electronic control of its hydrogen bonding ability and basicity (Fig. 2). Our initial aim was thus to prepare a range of guanidine catalysts.

Preparation of the studied catalysts

The catalysts initially investigated were prepared by the coupling of the *N*-alkylated-L-proline **23a–d** derivatives with alkyl, acyl or aryl substituted guanidines (see ESI†) using CDI as a coupling reagent in DMF (Scheme 3). This reagent was employed, as several other reagent combinations that were tested (DCC/NHS, DCC/HOBT, HBTU, $MeOCOCl/NEt_3$), were found to be ineffective and gave considerable problems on attempted purification. We initially attempted the preparation of the benzoyl substituted catalyst **24** and the crude compound was obtained, however on attempted purification it underwent hydrolysis on contact with moisture to give the parent benzoyl guanidine. This was somewhat worrying as if the other guanidines are prone to hydrolysis this might limit the use of these compounds. We next attempted the coupling of *N*-Cbz-guanidine and were pleased to obtain the compounds **25a–d** in good yields after chromatography. We similarly prepared the diphenyl substituted catalysts **26a–d** and found that the yields were good for the isopropyl- and cyclohexyl-substituted compounds whilst the methyl and benzyl were poor. The observation that coupling of *N*-methyl-L-proline **23a** under mixed-anhydride and other peptide coupling methods is problematic has been made by Lygo and Moore[12] who did not offer a clear insight as to why this was so, however our work might offer a possible explanation. The phenyl-substituted catalysts **27a-b** were also prepared in reasonable yield using method B in which the guanidine is generated *in situ* from a guanidinium salt and sodium hydride. We next attempted the preparation of the potentially more basic guanidines **28a–d**, from 1,1-dimethyl guanidine, using method B. On analysis of the crude reaction mixture of this reaction by proton NMR, the reactions appeared to be successful as the products were present. However, on work up we found that the products were highly polar and difficult to separate from the by-products of the reaction. In particular, the *N*-methyl substituted catalyst **28a** had a high water solubility/instability and was not isolatable if an aqueous work up was employed. In the case of the *N*-benzyl substituted **28b**, a low yield of the desired product was obtained as was a low yield of the dimeric compound **28e**. For reasons to be discussed later, the focus of catalyst preparation switched to the *N*-methyl substituted prolines and we next prepared the substituted

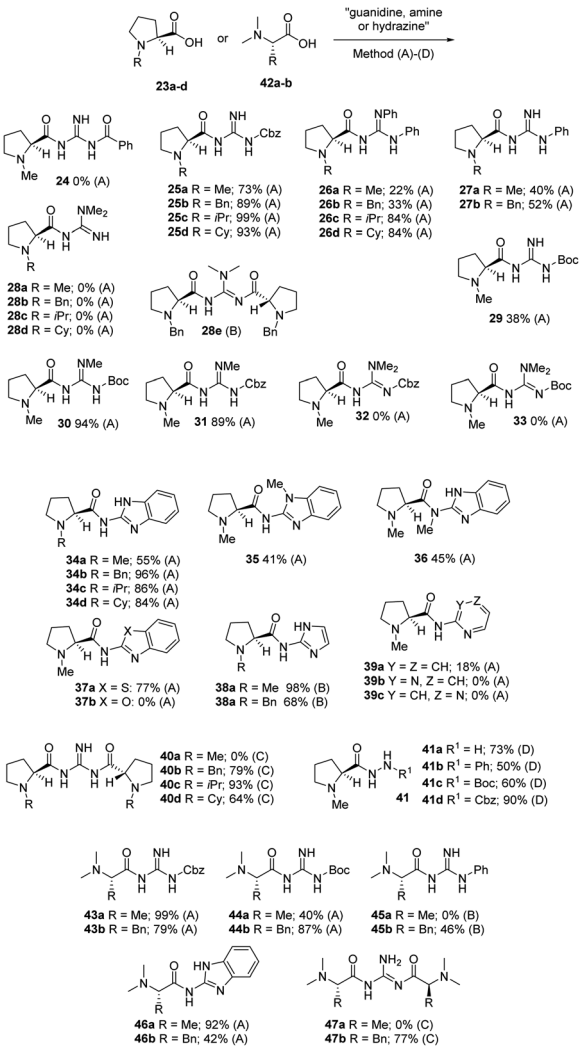

Scheme 3 Synthesis of the studied catalysts; conditions (A) **23a-d** or **42a-b**, CDI, DMF, rt, 24h. (B) (i) **23a-d** or **42a-b**, CDI, DMF, rt, 24h, (ii) guanidine. HX (X = Cl, HCO_3, NO_3), NEt_3. (C) (i) **23a-d**, CDI, DMF, rt, 24h, (ii) guanidine hydrochloride (0.5 equiv.), NaH (0.6 equiv.) DMF, rt, 24h. (D) (i) **23a**, AcCl, MeOH, 0 °C 1h, (ii) reflux, 12h, (iii) NH_2NHR^1, rt, 24h. R = Me, Bn, iPr, Cy; R^1 = H, Ph, Boc, Cbz.

guanidines **29** (*N*-Boc), **30** (*N*-Me, *N*′-Boc) and **31** (*N*-Me, *N*′-Cbz) by method A in good to excellent yields. We also attempted the preparation of the 1,1-dimethyl substituted Cbz **32** and Boc **33** guanidines and found that there was no indication of the formation of these compound, as on work up only recovered guanidine starting material was observed. This would suggest that either the guanidines were not reactive enough to displace the imidazole in the coupling intermediate or that the products **32** and **33** were hydrolysed during work up. We also prepared the benzimidazole derived prolines **34a–d** in good yields using coupling method A with again the lowest yield being observed for the *N*-methyl substituted **34a**. Similarly we prepared the methyl substituted benzimidazoles **35** and **36** in 41% and 45% yield respectively. We also prepared the benzothiazole **37a** catalyst in 74% yield using method A, however the benzoxazole **37b** was not accessible by this method which might be due to the low nucleophilicity of 2-aminobenzoxazole. Similarly the *N*-methyl **38a** and the *N*-benzyl-imidazole catalyst **38b** were prepared using the standard method in 97% and 68% yield respectively. We also attempted to prepare other heterocyclic derived catalysts with limited success. The pyridine derived catalyst **39a** was prepared using the CDI coupling method but the yield obtained (18%) was poor. Unfortunately, the pyrimidine **39b** and pyrazine **39c** derivatives could not be prepared using these conditions. We next attempted the preparation of the bis-L-proline substituted guanidines **40a–d** (method C) and found that the catalyst **40b–d** were formed in good to excellent yields. It was also observed that catalyst **40a** appeared to be formed under the conditions of the reaction as evidenced by proton and carbon NMR, however the product was lost on aqueous work up or on chromatography. This appeared to be due to a combination of factors including high water solubility and decomposition on silica gel and in water. The hydrazine derived *N*-methyl-L-proline catalysts **41c-d** were also prepared in good yields by esterification of *N*-methyl-L-proline **23a** with methanolic HCl followed by reaction with the corresponding hydrazine.

We also prepared a range of *N*,*N*-dimethyl alanine substituted guanidines (**43a–47a**) and also *N*,*N*-dimethyl phenylalanine substituted guanidines (**43b–47b**) using the previously employed CDI coupling method (Scheme 3). The Cbz-substituted **43a-b** and Boc-substituted guanidines **44a-b** were easily prepared in generally high yields. In the case of **44a**, the slightly lower yield might be due to problems associated with the aqueous work up as significant losses were observed. The phenyl-substituted guanidines **45a-b** were also prepared using the CDI coupling method with phenylguanidinium nitrate and hydrochloride, however compound **45a** was a very polar material and proved impossible to purify from polar organic and inorganic by products. Compound **45b** was less problematic and was purified by chromatography to give a moderate yield (46%). The benzimidazole substituted guanidines **46a** and **46b** were similarly prepared using this method in 92% and 42% yields respectively. The preparation of the symmetric disubstituted catalysts **47a** and **47b** was also attempted and again the L-alanine derived **47a** could not be obtained in a pure form which again appeared to be due to high aqueous solubility/instability. Pleasingly the phenylalanine derived compound **47b** was obtained in 77% yield under identical conditions after chromatography.

Michael addition reaction of 2-hydroxy-1,4-napthoquinone 1 with β-nitrostyrene 2

With these catalysts in hand we investigated the Michael addition reaction of 2-hydroxy-1,4-napthoquinone **1** with β-nitrostyrene **2** which in our hands had proven to be a robust reaction with little evidence of competing side reactions (Scheme 4a–c).

The catalysts **25a–d**, were initially investigated (Scheme 4a) and were pleased to see that all of these guanidines were effective catalysts leading to good conversions over 1–5 d as evidenced by NMR sampling of the reaction mixtures. We were pleased to observe some level of asymmetric induction (18–44%

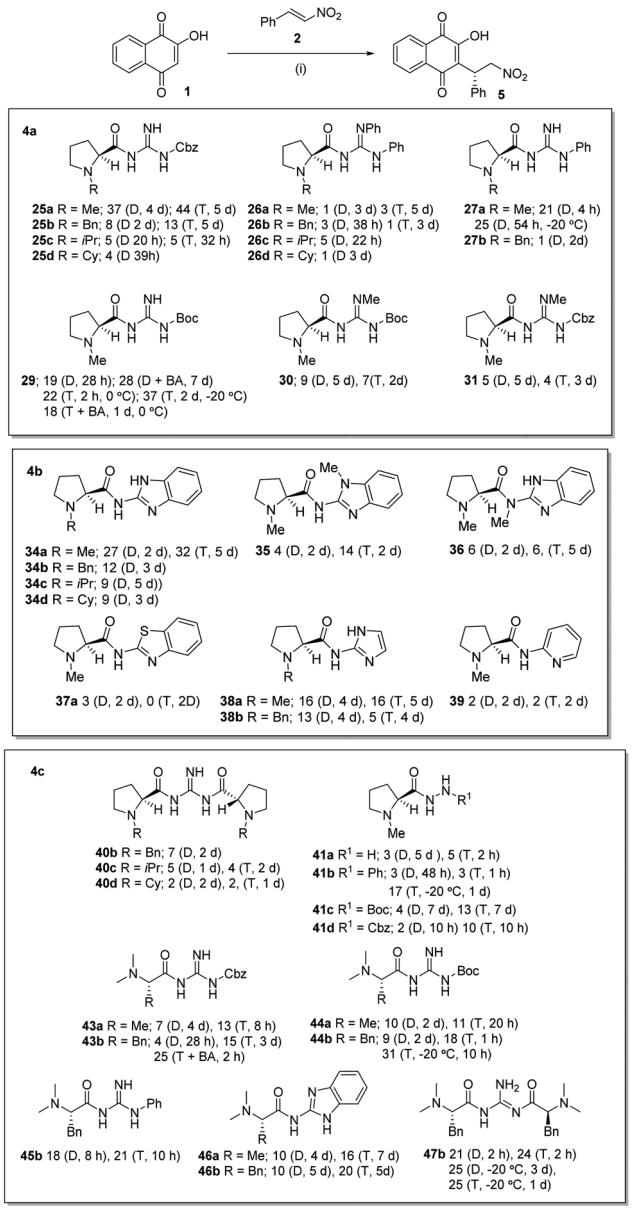

Scheme 4 (a–c): Catalyzed Michael reaction between **1** and **2**: conditions (i) catalyst (0.1–0.04 equiv.), solvent (0.03–0.08 M), −78 to 0 °C 7–8 h, then 0 °C-rt. Results are given as ee (solvent, time); D = dichloromethane, T = toluene.

ee) with all the catalyst with **25a** being the most effective. The highest ee was obtained using toluene as solvent, giving the product in 44% ee over 5 days and in a 75% isolated yield. Various solvent systems (CH_2Cl_2, MeCN, PhMe, THF, EtOAc and benzene) were studied, with the best results being obtained in dichloromethane and toluene. Using toluene presented some solubility problems associated with the starting material **1**, which was overcome by performing the reaction at higher dilution. It was also apparent that the catalytic reactions using **25a–d** were generally slow with 88–100 h being required for a reasonable conversion. It was also apparent that whilst all these compounds catalyzed the reaction, there was a steady decrease in ee as the size of the L-proline N-substituent increased from Bn to iPr to Cy. The diphenyl-substituted catalysts **26a–d** were investigated next (Scheme 4a) and whilst these compounds were found to catalyze the reaction at a similar rate to **25a–d**, the ee's of the product were consistently very low (1 to 5% ee) and at this point in the investigation we had no clear explanation for this. We next investigated the *N*-alkylated-benzimidazole prolines **34a–d** (Scheme 4b) and the results obtained with these catalysts were similar to those reported for **25a–d**. It was found that the *N*-methyl catalyst **34a** gave the highest levels of asymmetric induction with a 32% ee in toluene and a 27% ee in dichloromethane, however again there was a steady decrease in ee as the size of the proline *N*-substituent increased from Bn to iPr to Cy. We concluded from these studies that the size of the *N*-substituent on the proline is critical and that larger substituents appeared to detrimental to the ee of the reaction. We next investigated the mono-phenyl substituted catalysts **27a** and **27b** (Scheme 4a) and again the *N*-methyl substituted catalyst **27a** gave the best asymmetric induction. Interestingly and in contrast to the previous catalysts, the reaction time using **27a** in dichloromethane was shorter, leading to a 91% yield of **5** over 4 h with an ee of 21%. We repeated this reaction at −20 °C and obtained a slightly improved 25% ee over 54 h. This result was in stark contrast to the previous catalysts and we had no clear explanation for this at this point in the investigation. Again increasing the size of the N-substituent to a Bn group was detrimental to the ee as catalyst **27b** gave no appreciable levels of asymmetric induction in any of the solvents studied. We also investigated the Boc-substituted guanidine **29** (Scheme 4a) which gave a 19% ee in dichloromethane over 28 h and on the addition of benzoic acid as a co-catalyst the ee improved to 28%. Interestingly the reaction with **29** in toluene at 0 °C was rapid when compared to previous catalysts leading to an 89% yield of the product in 22% ee over 2 h. Repeating this experiment at −20 °C for 24 h gave an improved 37% ee but a lower yield (37%). Repeating the reaction in the presence of benzoic acid in toluene over 24 h gave a diminished ee of 18% and a much lower yield (38%).

In an attempt to increase the basicity of the guanidine and to modify the intramolecular hydrogen-bonding (*vide infra*) in the catalysts, the *N*-methylated-*N*′-Boc catalyst **30** and the *N*-methylated-*N*′-Cbz catalyst **31** (Scheme 4a) were investigated. These catalysts both gave poor ee's and slower reaction times and yields in both toluene and dichloromethane when compared to catalysts **25a** and **29**. These results might indicate that increasing the basicity of the guanidine does not help the reaction process or that interfering with the hydrogen-bonding pattern at this position is detrimental. These results were mirrored in the reactions of the *N*-methylated benzimidazole catalysts **35** and **36** (Scheme 4b) when compared to **34a**. These compounds were found to catalyze the reaction but again yields and ee's were lower (6–14% ee) and reaction times generally slower. Two catalysts were prepared in which the guanidine was replaced by a benzothiazole **37a** and a pyridine **39a** and again these catalyzed the reaction but gave poor ee's and slow reaction times. The imidazole catalysts **38a** and **38b** (Scheme 4b) were both effective catalysts with **38a** leading to a **5** in 16% ee in

dichloromethane or toluene, whilst **39a** gave lower ee's of 13% and 5% ee in the respective solvents.

We next investigated the C_2-catalysts **40b–d** (Scheme 4c) and were disappointed to find that whilst catalyzing the reactions effectively the ee's of the products were very low (1–7%) in either toluene or dichloromethane. Interestingly adding benzoic acid to the reaction decreased the conversion time but no increase in ee was apparent (see ESI†). The hydrazine derived catalysts **41a–d** (Scheme 4c) were investigated next and it was found that unsubstituted hydrazine **41a** gave slow reaction times and poor ee's. By contrast phenyl-substituted hydrazine **41b** gave a more rapid reaction in toluene whilst the reaction was again slow in dichloromethane. Unfortunately, the ee's of these reactions were again very low (3% ee), however repeating the reaction of **41b** in toluene at −20 °C gave an improved ee of 17% but over a longer time (1 d). The Boc-substituted hydrazine **41c** gave much slower reaction times but an improved 13% ee with toluene as reaction solvent. This slower reaction time might be due to an electronic effect as reactions of the Cbz-substituted hydrazine **41d** were more rapid (10 h) but ee's were slightly lower (10% ee).

Moving on from the L-proline derived catalysts we examined those derived from L-alanine and L-phenylalanine. The *N*-Cbz-protected guanidines **43a** and **43b** (Scheme 4c) were investigated initially and these were found to be effective catalysts. Compound **43a** gave an ee of 7% in dichloromethane over 4 d and 13% in toluene over 20 h, whilst **43b** gave 4% ee in dichloromethane over 28 h and 15% ee in toluene over 3 d. The latter result was repeated using benzoic acid as a co-catalyst and this led to a faster conversion and an improvement in ee to 25%. Following this the *N*-Boc-protected guanidines **44a** and **44b** (Scheme 4c) were investigated initially and again were found to be effective catalysts. Compound **44a** gave an ee of 10% in dichloromethane over 2 d and 11% in toluene over 20 h, whilst **44b** gave 9% in dichloromethane over 2 d and an 18% ee in toluene over 1 h. The latter result was repeated at 0 °C over 10 h and gave product **5** in 31% ee. These results seem to suggest the bulkier benzyl group found in the L-phenylalanine catalysts gives a more effective catalyst. Moving to the phenyl-substituted catalyst **45b** (Scheme 4c), similar results were found with an ee of 18% in dichloromethane over 8 h and 21% in toluene over 10 h. The benzimidazole catalysts **46a** and **46b** (Scheme 4c) were similarly investigated and overall were found to be slower that the previously investigated cases. Thus **46a** gave an ee of 10% in dichloromethane over 4 d and 16% in toluene over 7 d, whilst **46b** gave 10% ee in dichloromethane over 5 d and 20% ee in toluene over 5 d. Finally the C_2-catalyst **47b** gave similar results with an ee of 21% in dichloromethane over 2 h and 24% ee in toluene over 2 h. These reactions were repeated at −20 °C and ee of 25% in dichloromethane was obtained over 3 d and a 25% ee in toluene over 1 d.

Our overall conclusions from this work appear to be that the *N*-methyl-L-proline derived catalysts give better ee's in the reactions and increasing the substituent in general has a detrimental effect on the ee. The best groups on the guanidine of these catalysts appears to be those with Cbz-, Boc-, phenyl and benzimidazole substituents, whilst diphenyl and methyl substituted variants of the Cbz-, Boc- and benzimidazole catalysts led to lower ee's. Throughout this work the best solvent for this reaction appears to be toluene (and other aromatic solvents; see ESI†) with dichloromethane also being effective, however acetonitrile and other solvents were not successful. Cooling of the more rapid reactions appears to increase the ee of the product however, yields are lower and reaction times are prolonged. Throughout this work several catalysts seemed to increase the rate of reaction leading to completion or near completion in 1–4 h instead of the more typical 2–7 days, particularly catalysts **27a**, **29** + BA, **40c** + BA, **40d** + BA, **41b**, **43b** + BA, **44b** and **47b**. The exact reason for this was unclear and we thus decided to investigate the catalysts further.

Crystallographic and racemization studies

From the beginnings of this project we were interested in the crystallographic nature of our catalysts as it was felt that this information might lead to an insight into the efficiency (or not) of the systems employed. The initial crystallographic work of the previous student on this project gave some insight into the H-bonding patterns observed in the *N*-methyl-L-proline catalysts **25a**, **26a**, **27a** and **34a** catalysts. Three of these catalysts **25a**, **26a** and **34a**, had a distinctive H-bonding pattern (Fig. 3), which consisted of a strong intramolecular H-bond between the amide protons (NH) and the pyrrolidine nitrogen (bond a) and a complementary NH-bond between the guanidine NH and the amide carbonyl (bond b). This pattern holds the amide at a *trans*-configuration (*E*-) and in compound **25a** we refer to this as *E*-abd as the carbamate has an H-bond to the guanidine NH_2. In the case of **26a** and **34a** where no carbamate is present the *E*-ab pattern is found. We reasoned that the H-bonds found in these structures might still be present whilst they are in solution and this explain why these bases are slow to catalyze the Michael reaction. Some NMR evidence is also available which demonstrated that the ^{13}C NMR data for compound **26a** shows distinctive individual signals for each phenyl suggesting that rapid interconversion between these two phenyls is not occurring on the NMR timescale. Some further evidence for this is found in the structure of the guanidine **27a** (Fig. 3), which differs in its H-bonding pattern in that the pyrrolidine amine (N1) is not intramolecularly H-bonded and only the carbonyl–NH bond (bond b; N3(H1)···O1 = 2.02 Å) is present as the amide is in the form of a *N*-methyleneamide; this is termed a *Free*-b type system. Whilst this evidence is tenuous, this difference in H-bonding might explain the increased reaction rate observed in the Michael addition reaction for compound **27a** (proceeded in a 91% yield over 4 h), which was rapid when compared to the timescale of the other catalysts (typically took 4–5 days to reach completion). Another interesting feature is that the N4-phenyl group found in catalyst **26a** appears to eclipse the nitrogen N1. Catalysts **26a–d** gave very poor ee's in their reactions to form **5** and this eclipsing of the N might be a contributing factor (Fig. 3).

However, the most surprising and somewhat troubling result from our crystallographic studies was observed when examining the structure of **26a** which was found to crystallize as

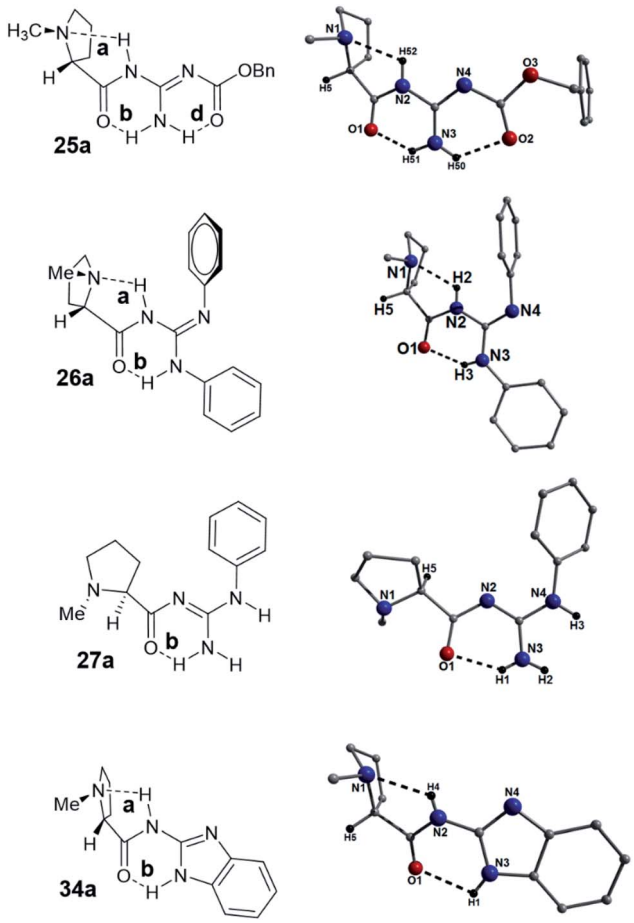

Fig. 3 ChemDraw representations (left) of catalysts **25a**, **26a**, **27a** and **34a** along with their corresponding crystal structures (right). Colour code as used throughout this work: C (grey), N (blue), O (red) and H (black). Dashed lines represent all intramolecular H-bonding interactions (N2(H52)···N1 = 2.26 Å, N3(H51)···O1 = 1.87 Å and N3(H50)···O2 = 2.00 Å in **25a**; N2(H2)···N1 = 2.15 Å and N3(H3)···O1 = 2.01 Å in **26a**; N3(H1)···O1 = 2.02 Å in **27a**; N2(H4)···N1 = 2.21 Å and N3(H1)···O1 = 2.35 Å in **34a**.

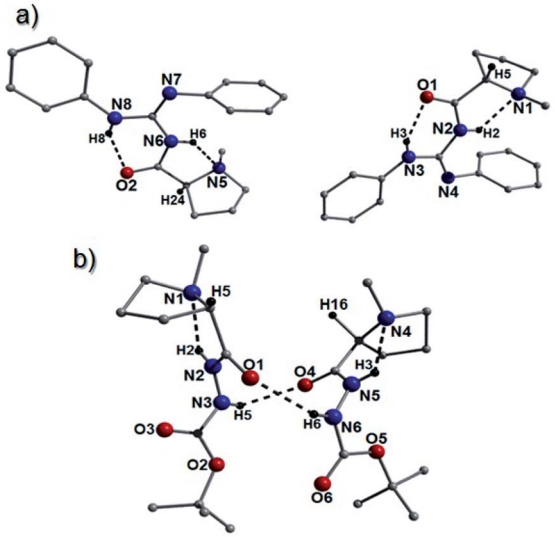

Fig. 4 (a) Crystal structure highlighting the two organic moieties (*S*-left and *R*-right) comprising the asymmetric unit in **26a**. The chiral protons are labelled H24 and H5. The dashed lines represent the intramolecular H-bonding interactions: N8(H8)···O2 = 2.03 Å; N6(H6)···N5 = 2.07 Å; N3(H3)···O1 = 2.01 Å and N2(H2)···N1 = 2.15 Å. Note: the disorder observed at both proline moieties is not shown. Catalyst **26a** crystallises as an 2 : 1 *S* : *R* epimeric mixture. (b) The asymmetric unit in **41c** (*crystal 1*). Dashed lines represent the intermolecular H-bonding (O1···(H6)N6 = 2.25 Å, N3(H5)···O4 = 2.18 Å) and intramolecular H-bonding (N2(H2)···N1A = 2.37 Å and N5(H3)···N4 = 2.20 Å).

a 2 : 1 (*S* : *R*) mixture of epimers within the unit cell (Fig. 4). Upon comparison with a simulated spectrum, the pXRD collection on **26a** was consistent with this observation (Fig. S25†). Similar racemization was observed in the crystal structures of compounds **41c** and **43a**. More specifically, the species **41c** was found to produce two types of crystal (*crystals 1* and *2*) within the same batch having crystallized in the $Pna2_1$ (**41c**-*crystal 1*) and $P2_1$ (**41c**-*crystal 2*) space groups. *Crystal 1* is racemic in nature (Fig. 4), while all **41c** units in *crystal 2* exhibit the *S* configuration (Fig. S22†). Interestingly, the simulated powder patterns obtained from *crystal 1* and *crystal 2* are virtually identical. Although they have almost identical unit cell dimensions (Table S5† and Fig. S26†), this also means there is significant correlation in how the species pack within a unit cell. Likewise, the bulk powder sample of **41c** also corresponds well to both simulated patterns. Unfortunately, the near identical nature of their simulated patterns severely hampers any attempts at obtaining a *crystal 1*/*crystal 2* ratio in **41c**. The catalyst **43a** also crystallized as a racemate (Fig. S23†).

This was a surprising observation, as the L-proline used in the synthesis was of the reported optical rotation, as was the *N*-methylproline **23a**, which was prepared using a literature procedure.[13] The epimerization of several of the catalysts was investigated by NMR in deuterated methanol under neutral, weakly basic (NEt_3) and acidic ($PhCO_2H$) conditions and whilst decomposition (hydrolysis) was observed over prolonged time-periods (>5 days), no evidence of deuterium incorporation at the proline chiral center was observed. We thus investigated the nature of the most successful catalyst **25a** by HPLC and found it to also be a 3 : 1 mixture of epimers by HPLC (by comparison with a separately prepared racemic sample). For compound **25a**, the PXRD patterns show observable differences. Realistically the only differences between the 86% ee and 100% ee patterns, is the sharpness of the peaks in the 100% ee (Fig. S28†). However they are both totally different from the racemic mixture, suggesting that the racemate has a completely different type of packing to the pure chiral form.

We concluded from this that the epimerisation must be occurring at the CDI coupling stage. We thus repeated the preparation of **25a** by coupling **23a** with *N*-Cbz-guanidine which was activated using CDI in DMF over different times. Analysis of the products by HPLC and optical rotation data was performed and the traces compared with an independently prepared racemic and enantiomerically pure sample of **25a** (obtained by repeated recrystallization) (Scheme 5, Table 1).

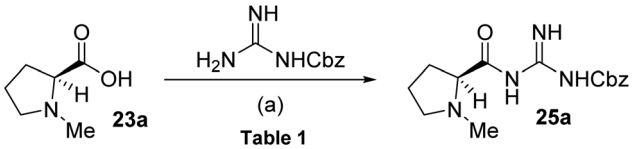

Time	HPLC	$[\alpha]_D$
5 Min	87% ee	-70 (92% ee)
60 Min	57% ee	-41 (54% ee)
24 h	33% ee	-24 (24% ee)

Scheme 5 (a) (i) **23a**, CDI, DMF, 5 min, 1 h or/24 h, rt; (ii) *N*-Cbz-guanidine, rt 24h; 47–53% yield.

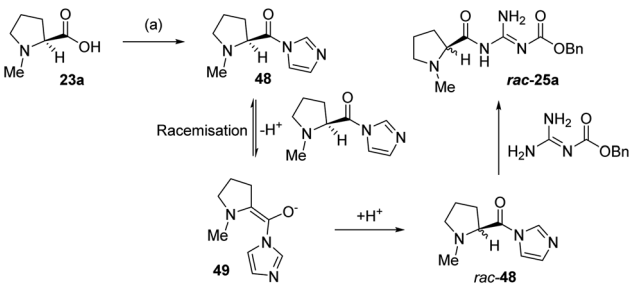

Scheme 6 Proposed mechanism for the racemization of the proline catalyst **25a**. (a) (i) CDI, DMF, (ii) *N*-Cbz-guanidine.

It was apparent from these experiments that even under short activation times racemization was occurring very rapidly. The only possible explanation of this is that the intermediate imidazole amide **48** was undergoing base catalyzed epimerization, *via* enolate **49**. The likely base for this process is the amide **48** itself and in the cases where relatively strong guanidine bases are used in the coupling, their presence might exacerbate this process (Scheme 6).

We thus repeated the preparation of the Michael adduct **5** using enantiomerically pure **25a** and were able to increase the ee of **5** to 56% ee over 48 h reaction in toluene. Similarly catalyst **29** was prepared using a short coupling time and repeated recrystallized to constant optical rotation and this again gave an increases ee for **5** to 41% (from 22%) over 10 h in toluene. These two compounds represent the best catalysts studied to date within this work.

Comparison of crystal H-bonding patterns and solution chemistry

We still wished to rationalize the reactions from the standpoint of the crystal structures and to this end, investigated the structures of several of the catalysts and were able to obtain crystallographic data on compounds **25a**, **26a**, **26c**, **26d**, **27a**, **29**, **30**, **31**, **34a**, **34b**, **34c**, **38b**, **39**, **40b**, **40d**, **41b**, **41c**, **43a**, **43b** and **44b**. As expected prior to their crystallization (and shown in Tables S1–S5†), the majority of our catalysts crystallized in Sohncke type space groups which include: $P1$ (**30**), $P2_1$ (**25a**, **26c**, **26d**, **29**, **34a**, **38**, **40d**, **41c** (*crystal 2*) and **43b**), $P2_12_12_1$ (**27a** and **40b**), $C222_1$ (**39**) and $P6_5$ (**34b**). On close inspection and as highlighted in Fig. 3–12 as well as throughout the ESI (Fig. S1–S24†), intramolecular hydrogen bonding is commonplace within each catalyst. More specifically, the majority of interactions occur between guanidine protons, neighboring carbonyl oxygen and proline nitrogen acceptor atoms (*e.g.* N7(H54)···O5 = 1.83 Å and (N6(H55)···N5 = 2.26 Å, respectively; Fig. 5).

We hoped to use the X-ray structures obtained to give some insight into the possible H-bonding patterns found in these catalysts in solution. We initially compared the X-ray structures of the compounds **25a**, **29**, **30** and **31**. Compounds **25a** and **29** have no methyl substituent on the guanidine and **25a** gave two H-bonds between the amide carbonyls and two of the N–H's of the guanidine (bond b; N3(H51)···O1 = 1.87 Å and bond d; N3(H50)···O2 = 2.00 Å). Additionally a H-bond between the proline nitrogen atoms (N1) and the amide NH (bond a; N2(H52)···N1 = 2.26 Å) was present and this compound was thus an *E*-abd type (Fig. 5).

The analogous Boc-protected compound **29** was prepared in order to study changes in steric factors near the guanidine and surprisingly it had a different H-bonding pattern (*E*-abc) to that of **25a**. Catalyst **29** had two H-bonds between the amide and the carbamate carbonyls and two of the N–H's of the guanidine (bond b; N3(H3)···O1 = 1.94 Å and bond c; N2(H1)···O2 = 2.09 Å). The H-bond between the proline nitrogen atom (N1) and the amide NH (bond a; N2(H1)···N1 = 2.10 Å) was also present (Fig. 6).

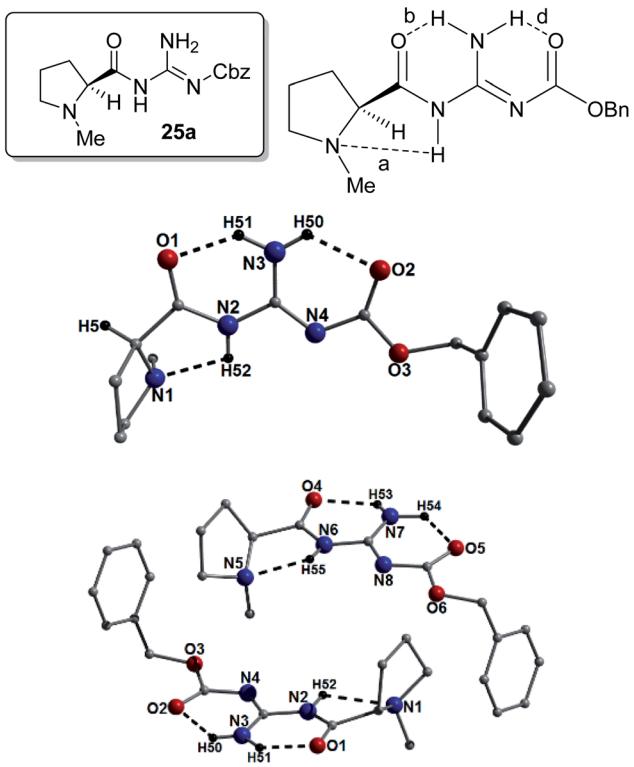

Fig. 5 ChemDraw (top) and crystal structure (middle) representations of **25a**. (Bottom): The two asymmetric units in **25a**. The dashes lines represent the intramolecular interactions within each moiety. These distances are: N2(H52)···N1 = 2.26 Å; N3(H50)···O2 = 2.00 Å; N3(H51)···O1 = 1.87 Å; N6(H55)···N5 = 2.26 Å; N7(H53)···O4 = 2.03 Å; N7(H54)···O5 = 1.83 Å. The longer contacts O2···H9A(C9) = 2.36 Å and O5···H24B(C24) = 2.33 Å are not shown.

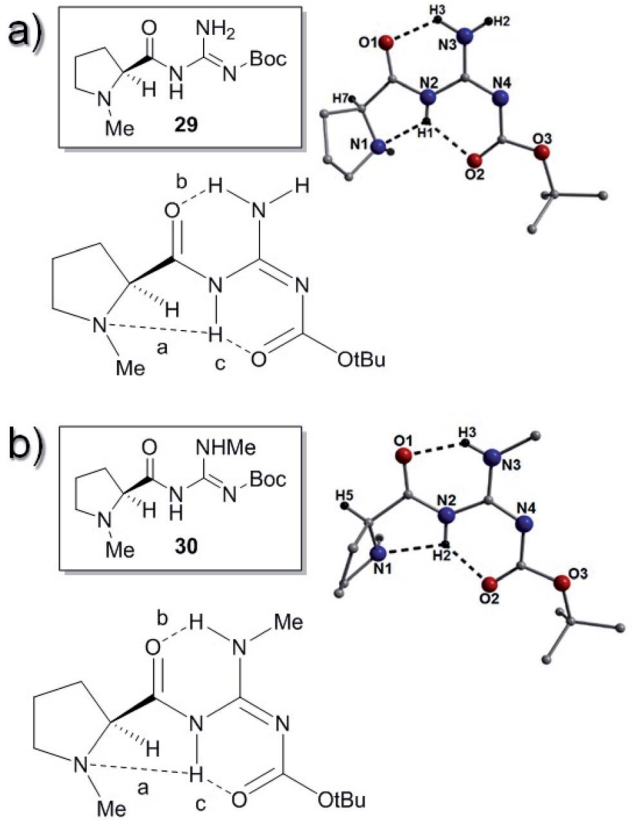

Fig. 6 (a) ChemDraw, H-bonding and crystal structure representations of **29**. The intramolecular H-bonding distances (dashed lines) are: N2(H1)···N1 = 2.10 Å, N2(H1)···O2 = 2.09 Å and N3(H3)···O1 = 1.94 Å. The chiral proton is labelled H7. Note: there are two units of **29** in the asymmetric unit and therefore only one is shown here. (b) ChemDraw, H-bonding and crystal structure of **30**. The intramolecular H-bonding distances (dashed lines) are 2.37 Å (N2(H2)···N1), 1.92 Å (N3(H3)···O1) and 1.92 Å (N2(H2)···O2). Note: there are two complete molecules in the asymmetric unit and so only one is shown here.

Compounds **30** and **31** were prepared in order to disrupt the intramolecular hydrogen bonding patterns in the catalysts. Catalyst **30** gave a structure with an identical H-bonding pattern (*E*-abc) to catalyst **29** as it had two H-bonds between the amide carbonyls and two of the N–H's of the guanidine (bond b; N3(H3)···O1 = 1.92 Å and bond c; N2(H2)···O2 = 1.92 Å). The H-bond between the proline nitrogen atom (N1) and the amide NH (bond a; N2(H2)···N1 = 2.37 Å) was also present (Fig. 6).

On close inspection of the X-ray crystal structure of compound **31**, more evidence of the proposed racemization process was observed as the unit-cell was shown to comprise a 2 : 1 mixture of *S* : *R* enantiomers. The powder X-ray diffraction spectrum obtained from **31** was found to compare favourably with the corresponding simulated spectrum generated by single crystal data (ESI, Fig. S29†). Despite this the *S*-enantiomer had an identical *E*-abc arrangement to **29** with two H-bonds between the amide carbonyls and two of the N–H's of the guanidine (bond b; N7(H34)···O4 = 1.90 Å and bond c; N6(H33)···O5 = 1.95 Å). The H-bond between the proline nitrogen atom (N5) and the amide NH (bond a; N6(H33)···N5 = 2.44 Å) was also still present (Fig. 7a).

It was observed that both catalyst **30** and **31** gave very slow reaction times and very low ee's in all the solvents studied and might indicate that substituting the hydrogens on the guanidine leads to a lowering of ee, possibly because we are blocking a site for H-bonding interactions. Contrasting these results to catalyst **29**, which gave very rapid reaction times in toluene, the lack of a methyl group might enable the guanidine N3–H2 and N4 positions to form a bidentate interaction with the quinone **1** or the nitro-group of β-nitrostyrene **2** and promote the reaction.

We were unable to obtain any X-ray data on the methyl-substituted benzimidazoles **35** and **36**, however we were able to obtain a structure on the imidazole compound **38b** (Fig. 7b). Compound **38b** had an *E*-ab hydrogen bonding pattern and possessed a H-bond between the proline nitrogen and the amide HN bond (bond a; N2(HN2)···N1 = 2.36 Å) and a H-bond between the imidazole NH and the amide carbonyl (bond b; N4(HN4)···01 = 2.24 Å). The ee's for the reaction of this catalyst were low, which might be due to the effect of the *N*-benzyl group as the corresponding *N*-methyl catalyst **38a** gave slightly better ee's. The lower ee's might indicate that the benzimidazole ring plays a role in the better ee's achieved with the catalyst **34a**.

The pyridine catalyst **39** had a single H-bond (*E*-a) between the proline nitrogen and the amide HN bond (bond a; N2(HN2)···N1 = 2.29 Å). Reaction times were reasonable for this catalyst (48 h) which might reflect the basicity of the pyridine, however no appreciable ee's were observed in the reactions (Fig. 7c). The two C_2-symmetric catalysts **40b** and **40d** and were found to possess similar hydrogen bonding patterns (see Fig. 7d and e). In compound **40b**, one amide NH was H-bonding to the proline nitrogen (bond a; N4(H14)···N5 = 2.44 Å) and this hydrogen was also H-bonding to the other amide carbonyl (bond c/b′: N4(H14)···O2 = 1.99 Å). The amide carbonyl is also H-bonding to the guanidine NH_2 (bond b; N3(H12)···O3 = 1.99 Å). The other proline nitrogen is free of intramolecular H-bonds so this H-bonding interaction overall is an *E*-abc/*Free*-b arrangement (Fig. 7d). Similarly an identical H-bonding patterns was observed for **40d** in that one amide NH was H-bonding to the proline nitrogen (bond a; N4(H4)···N5 = 2.28 Å) and this hydrogen was also H-bonding to the other amide carbonyl (bond c/b′: N4(H4)···O1 = 1.93 Å). The amide carbonyl is also H-bonding to the guanidine NH_2 (bond b; N3(H3B)···O2 = 2.06 Å). Again the other proline nitrogen is free of intramolecular H-bonds so this H-bonding interaction is also an *E*-abc/*Free*-b arrangement (Fig. 7e).

In both **40b** and **40d** it is apparent that the proline nitrogen (labelled N5 in both cases) is not involved in intramolecular hydrogen-bonding and this might leave it free for base catalysed reactions. This observation might explain why several of the reactions of these catalysts took relatively short times to complete (24–48 h, Scheme 4c and appendix IV). Unfortunately it seems apparent that the relatively strong intramolecular H-bonds of the guanidine NH's and the carbonyls might preclude the formation of the bidentate H-bonding pattern we had hoped for. This, together with the known problems associated with bulky nitrogen substituent groups may have led to the poor ee's.

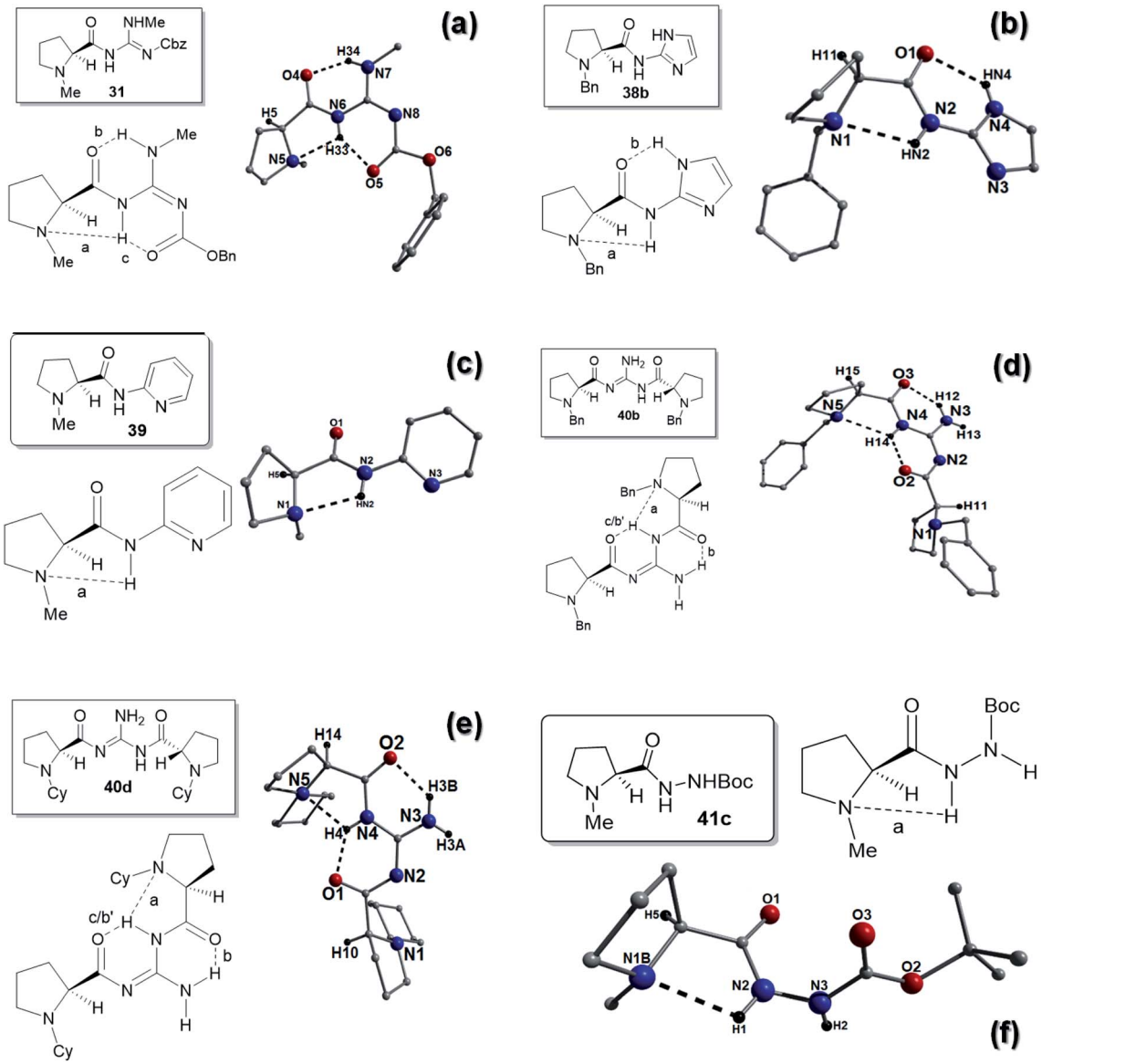

Fig. 7 ChemDraw and crystal structure representations of **31** (a), **38b** (b), **39** (c), **40b** (d), **40d** (e) and **41c** (f). All intramolecular H-bonding distances are represented as dashes lines. These distances are: (a) N6(H33)···N5 = 2.44 Å, N6(H33)···O5 = 1.95 Å, N7(H34)···O4 = 1.90 Å. (b) N2(HN2)···N1 = 2.36 Å, N4(HN4)···O1 = 2.24 Å. (c) N2(HN2)···N1 = 2.29 Å. (d) N4(H14)···N5 = 2.44 Å, N4(H14)···O2 = 1.99 Å, N3(H12)···O3 = 1.99 Å. (e) N4(H4)···N5 = 2.28 Å, N3(H3B)···O2 = 2.06 Å, N4(H4)···O1 = 1.93 Å. (f) N2(H1)···N1B = 2.32 Å. Note: **31** crystallises as an 2 : 1 *S* : *R* epimer mixture. The *S*-enantiomer is shown here. There are two types of crystals in the bulk material of **41c** (labelled *crystal 1* and *crystal 2*). *Crystal 1* is racemic in nature and all **41c** units in *crystal 2* exhibit the S configuration. The *S*-enantiomer extracted from *crystal 1* is shown in (f).

As previously stated the co-crystallisation of two polymorphs of **41c** (*crystal 1*: 1 : 1 racemic mixture and *crystal 2*: *S*-configuration only) indicated that the reaction has proceeded with partial racemization and that the 1 : 1 mixture has crystallized from a partially racemic mixture together with the *S*-enantiomer. Despite this a similar H-bond between the proline nitrogen and the amide HN bond (bond a; N2(H2)···N1 = 2.23 Å) was observed (*E*-a type) on examination of the *S*-enantiomer. This was shorter than that found in other catalysts, which might explain the slow reaction times for this compound compared to the other hydrazine catalyst (Fig. 7f).

The X-ray structure was also obtained for the phenyl hydrazine catalyst **41b** and was found to crystallize as a 2 : 1 mixture of the *S*- and *R*-enantiomers again indicating partial racemization or preferential crystallization. The powder XRD data obtained from a polycrystalline sample of **41b** suggests that its single crystal data is representative of the bulk sample (Fig. S30†). The H-bond pattern is similar to the majority of the guanidine catalysts in that it is an *E*-amide-ab′ type arrangement. As such, there is a H-bond between the nitrogen and the amide NH bond (bond a; N2(H2)···N3 = 2.29 Å) and a long H-bond between the amide carbonyl and the other NH of the hydrazine (bond b′; N1(H1)···O1 = 2.68 Å). This catalyst gave a very short Michael reaction time (1 h in toluene, xylene and benzene) and may be explained by the presence of the hydrazine PhNH, which will be more basic than the examples where this

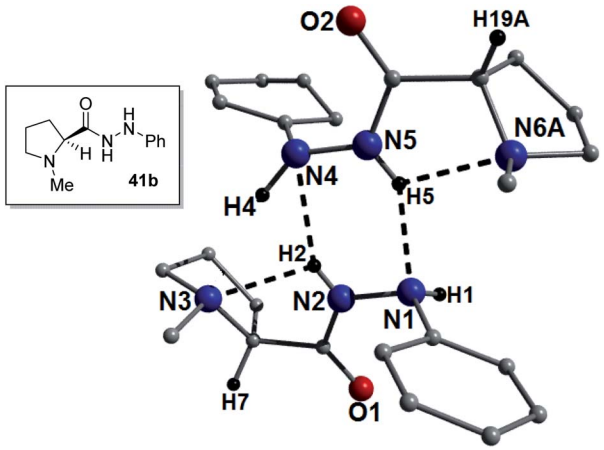

Fig. 8 ChemDraw (inset) and crystal structure representations of **41b**. The dashed lines represent intra- and intermolecular H-bonding interactions with distances: N2(H2)···N3 = 2.29 Å, N5(H5)···N6A = 2.30 Å, N2(H2)···N4 = 2.26 Å and N5(H5)···N1 = 2.18 Å. Note: the A label denotes a disordered (*R* : *S*) proline unit (only A is shown here). For clarity the N1(H1)···O1 intramolecular interaction is not shown here.

NH is a carbamate. Low ee's (2–3%) were obtained using this catalyst, however, on cooling the ee in toluene was improved to 17% (Fig. 8).

X-Ray structures of the dimethyl-L-alanine catalyst **43a** and the dimethyl-L-phenylalanine catalysts **44a** and **44b** were also obtained. Again, unfortunately, the dimethyl-L-alanine catalyst **43a** crystallized as a racemic mixture (single crystal and pXRD corroborate batch uniformity; ESI, Fig. S31†), however the *S*-enantiomer gave an *E*-abc type with H-bonds between the N–H of the amide and the dimethylamine together with an H-bond between a guanidine NH and the amide carbonyl (bond a; N3B(HN3)···N4 = 2.30 Å and bond b; N2(HN2A)···O3B = 2.05 Å). A third H-bond between the amide NH and the carbonyl of the Cbz groups was also observed (bond c; N3B(HN3)···O2 = 1.96 Å), which was the shortest H-bond of the three (Fig. 9).

The structure of the dimethyl-L-phenylalanine-phenyl guanidine catalyst **43b** was obtained and this had a significantly different *Free*-b type H-bonding pattern. In this structure the amide was present as an *N*-methyleneformamide which lacks an N–H bond. The only intramolecular H-bond was between the guanidine NH_2 and the amide carbonyl (bond b; N7(H7A)···O2 = 1.98 Å) (Fig. 12).

The dimethyl-L-phenylalanine catalyst **44b** gave no signs of racemization in the crystal. This compound displayed an *E*-abd H-bonding pattern with a hydrogen bond between the N–H of the amide and the dimethylamine together with a H-bond between a guanidine NH and the amide carbonyl (bond a; N3(HN3)···N4 = 2.48 Å and bond b; N2(HN2B)···O3 = 2.03 Å). A third H-bond was again observed, this time between the guanidine NH_2 and the carbonyl of the Cbz group (bond c; N2(HN2A)···O2 = 1.98 Å), which again was the shortest H-bond of the three (Fig. 9).

The Michael reaction using the dimethyl-L-alanine catalyst **43a** gave poor ee's (7–13%), over relatively long reaction times

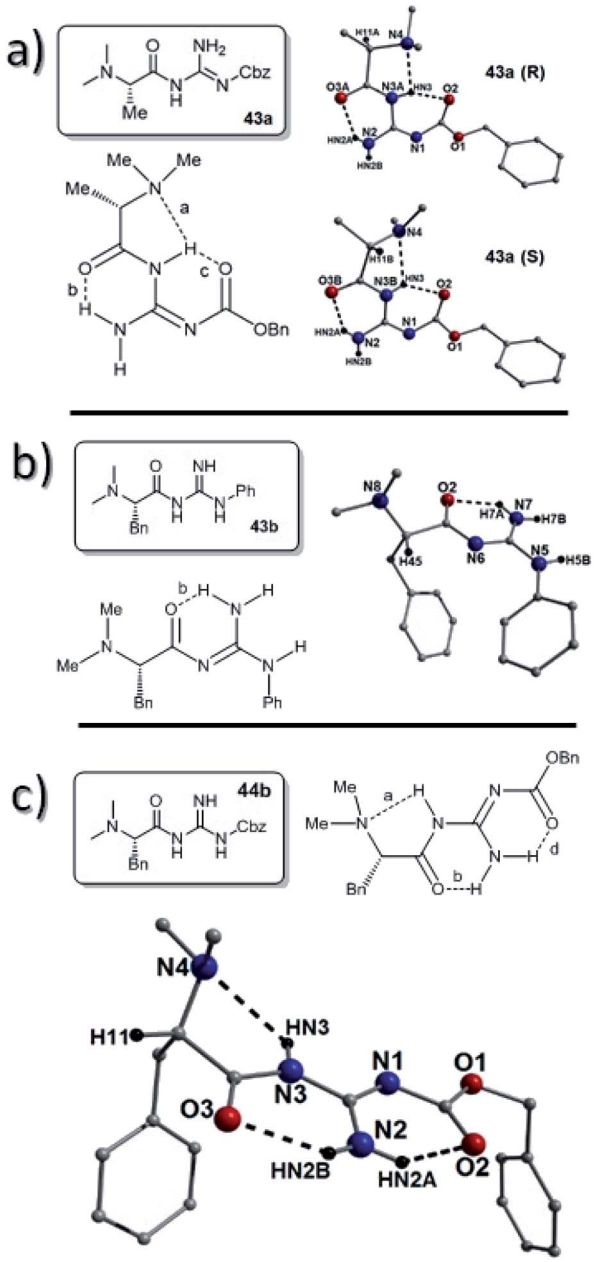

Fig. 9 (a) The ChemDraw representation and crystal structures of the *R*- and *S*-enantiomers observed in the racemic compound **43a**. Intramolecular H-bonding shown using dashed lines at distances: N2(NH2A)···O3A = 2.06 Å, N3A(HN3)···N4 = 2.30 Å and N3A(HN3)···O2 = 1.96 Å (in *R*) and N2(HN2A)···O3B = 2.05 Å, N3B(HN3)···2.30 Å and N3B(HN3)···O2 = 1.96 Å (in *S*). (b) ChemDraw and crystal of catalyst **43b**. The dashed lines represent intramolecular H-bonding interactions (N7(H7A)···O2 = 1.98 Å). Note: there are four molecules of **43b** in the asymmetric unit. A solitary unit is shown here. (c) Crystal structure obtained from **44b**. The dashed lines represent intramolecular H-bonding at distances: N2(HN2B)···O3 = 2.03 Å, N2(HN2A)···O2 = 1.98 Å and N3(HN3)···N4 = 2.48 Å.

(18–96 h). This might be a reflection on the degree of racemisation or possibly the level of H bonding. The dimethyl-L-phenylalanine catalyst **44b** gave better ee's (4–25%) but again generally relatively long reaction times. In contrast, the

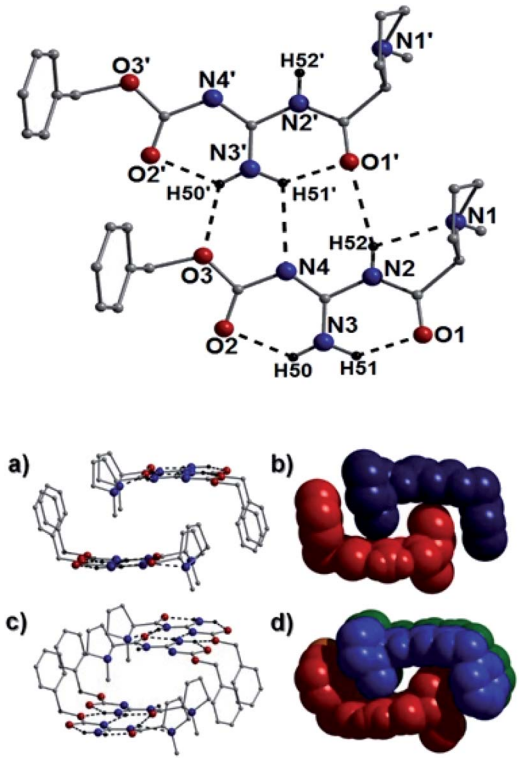

Fig. 10 (Top): Intermolecular H-bonding arrangement (dashed lines) between two crystallographically equivalent **25a** units. Selected distances: O3···(H50′)N3′ = 2.20 Å; N4···(H51′)N3′ = 2.63 Å and N2(H52)···O1′ = 2.58 Å. Note: intramolecular H-bonding also shown (dashed lines). (Bottom): Regular (a and c) and space-fill (b and d) views of the packing arrangement observed in **25a**. Each unit (in b and d) is represented by a different colour to highlight the space efficient interdigitation of the U-shaped organic units in **25a**.

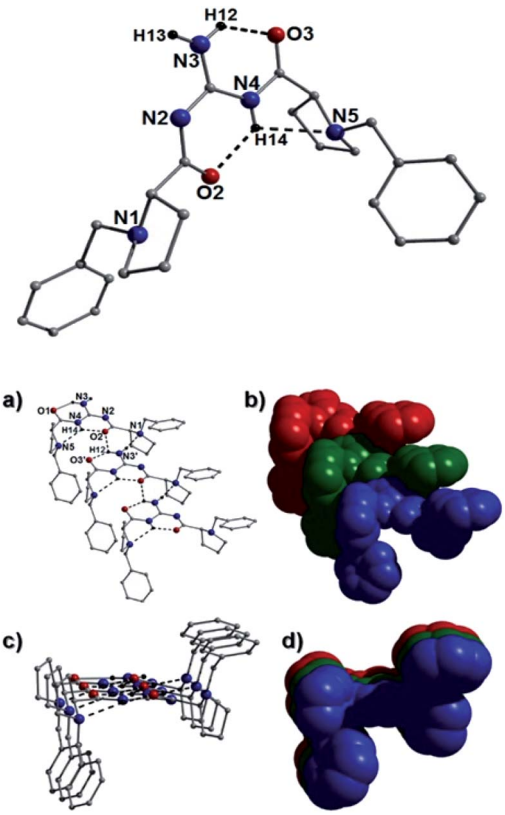

Fig. 11 (Top): The crystal structure of **40b**. The dashed lines represent the intramolecular hydrogen bonding interactions: N4(H14)···O2 = 1.99 Å; N3(H12)···O3 = 1.99 Å and N4(H14)···N5 = 2.44 Å. (Bottom): A section of the H-bonded (dashed lines) chains in **40b** as viewed off-set (a) and parallel (c) to the plane of the H-bonded guanidine moieties along with their space-fill representations (b and d respectively). The individual guanidine units are colour coded. The intermolecular H-bonded distances are: N1···(H13′)C13′ = 2.06 Å (not shown); O2···(H12′)N3′ = 2.40 Å and C17(H17A)···O3′ = 2.80 Å.

dimethyl-L-phenylalanine phenyl guanidine catalyst **43b** gave rapid reaction times (8–10 h) in all solvents and the ee's (18–21%) were high when compared to the other two catalysts. This might possibly be due to the more basic nature of the guanidine, which is substituted with only one electron withdrawing carbonyl containing group. These observations might suggest that the presence of the carbamate protecting groups is detrimental to the efficiency of the reaction and does not lead to a high ee product (as previously postulated).

Whilst it is difficult to draw conclusions from the X-ray data, it is obvious the presence of racemization is a major concern in the potential for these catalysts. Despite this there is some evidence that the more substituted catalysts are less efficient and that a maximum of two substituents seems to be the most promising. Some interesting observations were also made regarding intermolecular H-bonding interactions and this is discussed below.

Intermolecular interactions

In terms of intermolecular interactions and as exampled by the species **25a**, **40b** and **43b**, the individual organic moieties in a number of our catalysts self-assemble in the solid-state as planar sheet arrays through complementary H-bonding interactions as highlighted in Fig. 10 (**25a**), Fig. 11 (**40b**) and Fig. 12 (**44b**). In all these examples, the H-bond connections are forged through guanidine protons and neighboring carbonyl oxygen, alcohol oxygen and/or guanidine nitrogen acceptor atoms (*i.e.* N2(H52)···O1′ = 2.58 Å and N4···(H51′)N3′ = 2.63 Å in Fig. 10). For example, the catalyst **25a** comprises two organic crystallographically unique moieties within its asymmetric unit and partake in side-on C–H···π intermolecular interactions between proline protons and juxtaposed benzoate aromatic rings (*e.g.* C17(H17B)···[C10–C15] = 3.01 Å and C2(H2B)···[C25–C30] = 3.20 Å) to form an interdigitated rectangular dimeric assembly. Likewise, intermolecular complementary H-bonding between the individual guanidine units connect these dimeric units along the *a* unit cell direction to form tubular sheet-like arrays throughout the crystal structure in **25a** (Fig. 10).

Akin to the connectivity arrangements in **25a**, the chair-shaped organic units in **40b** produce superimposable H-bonded sheets along the *a* unit cell direction (Fig. 11). The intermolecular hydrogen bonding interactions are forged between guanidine protons and neighbouring carbonyl oxygen acceptor atoms (*e.g.* N3(H12)···O2′ = 2.40 Å). The individual H-

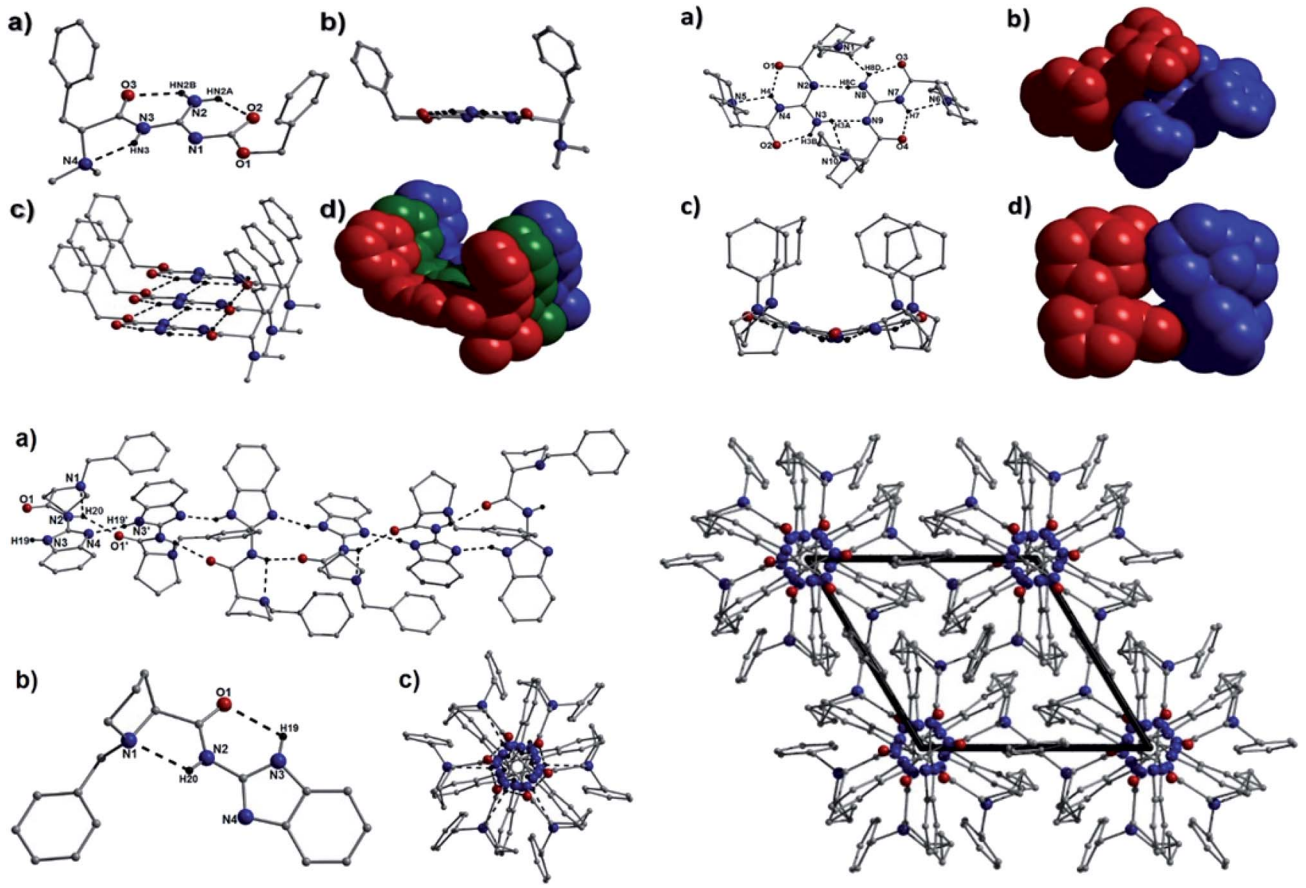

Fig. 12 (Top left): Crystal structure of **44b** highlighting (a) the intramolecular H-bonding interactions in **44b** (dashed lines) (N3(HN3)···N4 = 2.48 Å; N2(HN2A)···O2 = 1.98 Å and N2(HN2B)···O3 = 2.03 Å) and (b and c) the superimposable U-shaped 1D H-bonded rows of **44b** units propagating along the *a* direction of the unit cell. Selected intermolecular H-bonding interactions: N3(HN3)···O3′ = 2.54 Å; N1···(HN2B′)N2′ = 2.49 Å and O1···(HN2A′)N2′ = 2.22 Å. (d) is a space-fill representation of the 1D rows in **44b**. Each colour represents a single organic unit. (Top right): Crystal structure of the dimeric asymmetric unit **40d** as viewed perpendicular (a) and parallel (c) to the plane of the H-bonded (dashed lines) guanidine moieties along with their colour coded space-fill representations (b and d, respectively). Intramolecular H-bonded distances: N3(H3B)···O2 = 2.06 Å; N4(H4)···O1 = 1.93 Å; N8(H8D)···O3 = 2.05 Å; N7(H7)···O4 = 1.95 Å; N7(H7)···N6 = 2.31 Å and N4(H4)···N5 = 2.28 Å. Intermolecular H-bonded distances: N8(H8C)···N2 = 2.11 Å; N3(H3A)···N9 = 2.09 Å; N3(H3B)···N10 = 2.89 Å and N8(H8D)···N1 = 2.96 Å. (Bottom left): (a) A H-bonded helical chain of individual units of **34b** propagating along the *c* unit cell direction. The dashed lines represent the intermolecular H-bonding interactions in **34b** (N2(H20)···O1′ = 2.26 Å and N4···H19′(N3′) = 2.02 Å). (b) The asymmetric unit in **34b** highlighting (dashed lines) the intramolecular H-bonding interactions (N2(H20)···N1 = 2.33 Å and N3(H19)···O1 = 2.36 Å). (c) A single H-bonded helical chain in **34b** as viewed along the *c* direction of the unit cell. (Bottom right): Crystallographic packing of **34b** as viewed along the *c* direction of the unit cell.

bonded rows in **40b** connect along the *bc* plane of the unit cell through C–H···π interactions between proline protons and neighbouring aromatic rings at distances of (for instance): 3.83 Å (C15(H15)···[C20–C25]), 3.46 Å (C15(H16B)···[C20–C25]) and 3.44 Å (C17(H17B)···[C20–C25]). In a similar fashion, the individual U-shaped organic units in **44b** connect along the *a* cell direction *via* numerous intermolecular interactions to form a H-bonded half pipe array as highlighted in Fig. 12.

In a similar vein, the catalysts **29**, **30** and **40d** arrange into H-bonded dimers and are presumably too sterically hindered by their *tert*-butyl (**29** and **30**) and cyclohexane (**40d**) groups to forge planar sheet topologies as previously described. For instance, the catalyst **40d** crystallises in the monoclinic $P2_1$ space group (screw axis along *b* cell direction) and exhibits two organic moieties in the asymmetric unit. Indeed these U-shaped guanidine moieties H-bond to one another *via* their guanidine protons (H3A and H8C) to form dimeric units that forge a U-shaped half-pipe motif as highlighted in Fig. 12.

Interestingly, the benzimidazole containing proline derived catalyst **34b** crystallises in the hexagonal $P6_5$ space group whose translational symmetry is manifested through the formation of H-bonded helical chains propagating along the *c* direction of the unit cell (Fig. 12-bottom left). These chains organise themselves into a space efficient brickwork motif to give the packing arrangement shown in Fig. 12 (bottom right). Moreover, the structurally related catalyst **34c** is the only member to encapsulate a solvent molecule during crystallisation. More specifically, a crystallographically unique water of crystallisation lies at H-bonding distance from the organic moiety in **34c**. This molecule is held in position through H-bonding with

a guanidine proton (H2N) at a distance of 2.15 Å (N2(H2N)···O2) and a guanidine N acceptor atom of an adjacent organic moiety at a distance of 2.09 Å (N4···(H20)O2) (Fig. S14 and S15†). As a result, these waters of crystallisation as molecular cement in connecting the individual brick units in **34c** as they propagate along the *a* unit cell direction (Fig. S16†).

Conclusions

The work presented here has illustrated that amino acid derived guanidine have some potential as asymmetric organocatalysts however several problems have arisen. Crystallographic investigation of the catalysts has led to the discovery of quite prevalent racemization occurring during their formation under CDI activated coupling. Obviously, this is a major drawback to their use as catalysts and they are not competitive in terms of producing the targeted asymmetric products. Our investigation in the solid state demonstrated extensive intra- and intermolecular H-bonding abilities of the proline, guanidine and/or amide functional groups within these organic moieties. These interactions lead to the production of elaborate and aesthetically pleasing hydrogen bonded extended network architectures. Consideration of the intramolecular H-bonding gave a loose correlation with catalytic efficiency and it inferred that these interactions remain in place in solution. A consideration of these structural interactions might lead the way to development of new catalysts. Indeed our current work addresses this together with new methodology to produce related catalysts without the problems associated with racemisation.

Experimental

General procedures

Unless otherwise noted, reactions were stirred and monitored by TLC. TLC plates were visualized using iodine, phosphomolybdic acid or under UV light. All anhydrous reactions were conducted under a static argon atmosphere using oven dried glassware that had previously been cooled under a constant stream of nitrogen. Reagents and starting materials were purchased from commercial suppliers and used without further purification unless otherwise noted. All anhydrous solvents used in reactions were distilled over either sodium wire and benzophenone (THF/DE) or calcium hydride (DCM), and used either immediately or stored over molecular sieves prior to use. Flash column chromatography was performed on Davisil® silica gel (35–70 microns) with the eluent specified in each case, TLC was conducted on precoated E. Merck silica gel 60 F_{254} glass plates. Melting points were determined using a Gallenkamp MF370 instrument and are uncorrected. ^{1}H and ^{13}C NMR spectra were recorded on a Bruker Avance 400 or 500 spectrometer with an internal deuterium lock at ambient temperature at 400 or 500 MHz with internal references of δ_H 7.26 and δ_C 77.016 ppm for $CDCl_3$, δ_H 3.31 and δ_C 49.0 ppm for CD_3OD and δ_H 2.54 ppm and δ_H 39.52 ppm for DMSO. All mass spectra were performed at the EPSRC National Mass Spectrometry Service Centre based in Swansea. Low resolution Chemical Ionisation (CI) and Electrospray Ionisation (ESI) mass spectra were recorded on a Micromass Quattro II spectrometer and high resolution mass spectra were recorded on either a Finnigan MAT 900 XLT or a Finnigan MAT 95 XP. Infrared samples were prepared as thin films or solutions using sodium chloride plates or as KBr discs; spectra were recorded on a Bruker Tensor 37 FT-IR. Optical rotations were determines on an ADP400 polarimeter. The *N*-alkylated prolines were prepared by literature methods and the guanidines and heterocycles used in the study were prepared by literature methods or are commercially available, full details of these preparations are given in the ESI.† All PXRD samples were collected on a Rigaku MiniFlex 600 (CuK_α radiation (40.0 kV, 15.0 mA), over a 2θ range of 5 to 40°.

General methods for the preparation of the catalysts 21–41 and 43–47

Method A. The *N*-alkyl-L-proline (1.0–1.6 equiv.) was dissolved in DMF (1–2.5 mL per mmol), CDI (1.2 equiv.) was added and the mixture stirred for 5 min to 24 h. After cooling (0 °C) the mixture, the required guanidine (1.0 equiv.) was added as a solid and the mixture stirred to rt over 16–168 h. After evaporation under reduced pressure (freeze dryer) or dilution with water and extracting with ethyl acetate, drying ($MgSO_4$) and evaporation under reduced pressure, the product was obtained and was purified by column chromatography (DE/PE or EA/PE), recrystallization, trituration or a combination of these techniques.

Method B. The *N*-alkyl-L-proline (1.0 equiv.) was dissolved in dry DMF (1–2.5 mL per mmol), CDI (1.2 equiv.) was added and the mixture stirred for 3–16 h. In a separate flask, sodium metal (1.0 equiv.) was added to methanol (1–2 mL per mmol) and after complete reaction, the phenylguanidinium salt (1.0 equiv.) was added and the solution stirred for 30 min. This mixture was evaporated under high vacuum to dryness and the activated proline solution was added to it *via* cannula. The resultant mixture was stirred for 5 days, then water (100 mL) was added and the mixture extracted with EA (3× 100 mL). Once combined, the extracts were washed with water (3× 500 mL), dried ($MgSO_4$) then evaporated under reduced pressure. Purification was by column chromatography (EA in PE), recrystallization, tritutation or a combination of these techniques.

Method C. (C_2-catalysts): the *N*-alkyl-L-amino acid (1 equiv.) and CDI (1.20 equiv.) were added sequentially to dry DMF (0.5–2.5 mL per mmol) and the mixture stirred for 1–16 h. In a separate flask, NaH (0.60 equiv.) was suspended in dry DMF (1.0–2.0 mL per mmol) and dried (over P_2O_5) guanidinium chloride (0.50 equiv.) was added. After stirring for 1 h the activated amino acid solution was transferred into this flask *via* cannula and the mixture stirred for 24–48 h. The mixture was diluted with water (100 mL) and EA (100 mL), separated and the aqueous layer extracted with further EA (2× 100 mL) and the combined extracts washed with water (2× 100 mL). After drying ($MgSO_4$) and evaporation under reduced pressure the residue was co-evaporated with heptane to remove residual DMF and purified by silica gel chromatography (EA in PE), recrystallization, tritutation or a combination of these techniques.

Method D: (*S*)-1-methylpyrrolidine-2-carbohydrazide 41a. *N*-Methyl-L-proline **23a** (2.30 g, 17.8 mmol, 1.0 equiv.) was dissolved in MeOH (10 mL), cooled (0 °C) and acetyl chloride (2 mL, 2.2 g, 28.0 mmol, 1.6 equiv.) was slowly added over 5 min. The mixture was heated at reflux for 12 h, cooled to rt and concentrated under reduced pressure. The residue was triturated with DE (3× 50 mL) and dried under vacuum to give (2*S*)-2-(methoxycarbonyl)-1-methylpyrrolidin-1-ium chloride (2.51 g, 14.0 mmol) as a brown gum in 79% yield. The crude ester (1.57 g, 8.77 mmol) was dissolved in MeOH (9 mL) and hydrazine hydrate (98%, 8.27 g, 0.165 mols, 8.1 mL, 9.3 equiv.) was added drop wise over 5 min. After stirring for 24 h, a white precipitate was removed by filtration and the filtrate concentrated under reduced pressure to give a yellow oily residue. Trituration of the residue with $CHCl_3$ (2× 40 mL) followed by drying under vacuum gave the crude product as a yellow oil (1.75 g) which was purified by column chromatography (5–10% MeOH in $CHCl_3$ with 1% NEt_3) to give **41a** (1.15 g, 8.03 mmol) as a pale yellow oil in 93% yield (73% over 2 steps).

Spectroscopic data

(*S*)-*N*-Cbz-*N*′-carbamimidoyl-1-methylpyrrolidine-2-carboxamide 25a: method A. *N*-Methyl-L-proline **23a** (0.50 g, 3.87 mmol, 1.0 equiv.); DMF (10 mL); CDI (0.75 g, 4.65 mmol, 1.2 equiv.); 3 h; *N*-Cbz-guanidine (0.74 g, 3.87 mmol, 1.0 equiv.); 27 h. Evaporation then column chromatography (0–60% DE in PE) gave **25a** (0.86 g, 2.82 mmol) as a white solid in 73% yield. R_f 0.17 (10% DE/PE); mp 67–70 °C; $[\alpha]_D^{21}$ −64.8 ($CHCl_3$, $c = 1.0$); δ_H ($CDCl_3$) 8.24–10.8 (3H, br. s, 2× NH), 7.38–7.44(2H, m, 2× CH), 7.26–7.38 (3H, m, 3× CH), 5.16 (H, d, *J* 12.9 Hz, CH), 5.12 (H, d, *J* 12.9 Hz, CH), 3.05–3.08 (1H, m, CH), 3.01 (1H, dd, *J* 4.8, 10.5 Hz, CH), 2.42 (1H, dd, *J* 6.5, 10.1 Hz, CH), 2.38 (3H, s, Me), 2.2–2.32 (1H, m, CH), 1.71–1.96 (3H, m, CH, CH_2); δ_C ($CDCl_3$) 178.0, 163.9, 158.8, 136.6, 128.4, 128.2, 128.0, 68.9, 67.0, 56.5, 41.7, 31.3, 24.6; ν_{max} (KBr disk) 3395, 3279, 3086, 2945, 1704, 1656, 1611, 1375, 1090 cm^{-1}; MS (EI) *m*/*z* 305.2 (100%, $M + H]^+$); HRMS (ESI) *m*/*z*, found 305.1610, $C_{15}H_{21}N_4O_3^+$ ($[M + H]^+$) requires 305.1608.

(*S*)-*N*-Cbz-1-benzyl-*N*′-carbamimidoylpyrrolidine-2-carboxamide 25b: method A. *N*-Benzyl-L-proline **23b** (1.0 g, 4.87 mmol, 1.0 equiv.); DMF (11 mL); CDI (0.95 g, 5.85 mmol, 1.2 equiv.); 3 h; Cbz-guanidine (0.95 g, 4.87 mmol, 1.0 equiv.); 48 h. Extraction and column chromatography (0–60% EA in PE) gave **25b** (1.63 g, 4.29 mmol) in 89% yield as a white solid. R_f 0.10 (20% EA/PE); mp 101–103 °C; $[\alpha]_D^{21}$ −67.1 ($CHCl_3$, $c = 1.0$); δ_H ($CDCl_3$) 7.93–11.30 (3H, br s, 3× NH), 7.21–7.29 (10H, m, 2× Ph) 5.20 (1H, d, *J* 12.4 Hz, CH), 5.15 (1H, d, *J* 12.4 Hz, CH), 3.74 (2H, s, CH_2), 3.29 (1H, dd, *J* 3.9, 10.3 Hz, CH), 3.06–3.19 (1H, m, CH), 2.45–2.56 (1H, m, CH), 2.18–2.33 (1H, m, CH), 1.69–1.97 (3H, m, CH, CH_2); δ_C ($CDCl_3$) 177.9, 163.5, 158.5, 136.7, 136.7, 129.5, 128.6, 128.4, 128.1, 128.0, 127.8, 67.0, 66.9, 59.7, 54.2, 31.0, 24.2; ν_{max} (KBr disc) 3381, 3059, 2938, 1703, 1652, 1607, 1553, 1404, 1118, 1028 cm^{-1}; MS (ESI) *m*/*z* 381.2 (100%, $[M + H]^+$); HRMS (ESI) *m*/*z* found 381.1914, $C_{21}H_{25}N_4O_3^+$ ($[M + H]^+$) requires 381.1921.

(*S*)-*N*-Cbz-*N*′-carbamimidoyl-1-isopropylpyrrolidine-2-carboxamide 25c: method A. Isopropyl-L-proline **23c** (1.0 g, 6.36 mmol, 1.0 equiv.); DMF (10 mL); CDI (1.24 g, 7.63 mmol, 1.2 equiv.); 4 h; Cbz-guanidine (1.23 g, 6.36 mmol, 1.0 equiv.); 16 h. Extraction, co-evaporation with heptane (4× 50 mL) and column chromatography (0–100% EA in PE) gave **25c** (2.09 g, 6.29 mmol) in 99% yield as a pale yellow oil. R_f 0.30 (80% EA/PE); $[\alpha]_D^{20}$ −31.1 ($CHCl_3$, $c = 1.0$); δ_H ($CDCl_3$) 7.62–11.45 (3H, br s, 3× NH), 7.25–7.44 (5H, m, Ph), 5.17 (1H, d, *J* 12.4 Hz, CH), 5.13 (1H, d, *J* 12.5 Hz, CH), 3.35 (1H, br d, *J* 10.5, CH), 3.12 (1H, t, *J* 7.5 Hz, CH), 2.73–2.81 (1H, m, CH), 2.49–2.57 (1H, m, CH), 2.07–2.17 (1H, m, CH), 1.89–1.98 (1H, m, CH), 1.73–1.81 (1H, m, CH), 1.62–1.73 (1H, m, CH), 1.07 (3H, d, *J* 7.4 Hz, Me), 1.06 (3H, d, *J* 7.0 Hz, Me); δ_C ($CDCl_3$) 179.7, 163.9, 158.7, 136.7, 128.5, 128.3, 128.0, 67.1, 64.5, 53.3, 50.9, 31.8, 24.7, 21.1, 20.1; ν_{max} (KBr disc) 3388, 3080, 2968, 1706, 1651, 1562, 1413, 1275, 1135 cm^{-1}; MS (ESI) *m*/*z* 333.2 (100%, $[M + H]^+$); HRMS (ESI) *m*/*z* found 333.1920, $C_{17}H_{25}N_4O_3^+$ ($[M + H]^+$) requires 333.1921.

(*S*)-*N*-Cbz-*N*′-carbamimidoyl-1-cyclohexylpyrrolidine-2-carboxamide 25d: method A. *N*-Cyclohexyl-L-proline **23d** (0.4 g, 2.03 mmol, 1.0 equiv.); DMF (5 mL); CDI (0.39 g, 2.43 mmol, 1.2 equiv.); 4 h; Cbz-guanidine (0.39 g, 2.03 mmol, 1.0 equiv.); 18 h. Extraction and recrystallization (ME/DE) gave **25d** (0.70 g, 1.88 mmol) in 93% yield as a pale yellow solid. R_f 0.19 (80% EA/PE); mp 167–168 °C; $[\alpha]_D^{16}$ −63.5 ($CHCl_3$, $c = 1.0$); δ_H ($CDCl_3$) 9.39–10.66 (1H, br s, NH), 8.26–9.39 (2H, br s, 2× NH), 7.39 (2H, br d, *J* 7.2 Hz, 2× CH), 7.32 (2H, br t, *J* 7.2 Hz, 2× CH), 7.27 (1H, br d, *J* 7.2 Hz, CH), 5.13 (1H, d, *J* 12.3 Hz, CH), 5.09 (1H, d, *J* 12.3 Hz, CH), 3.34 (1H, dd, *J* 2.4, 10.7 Hz, CH), 3.10 (1H, br t, *J* 7.4 Hz, m, CH), 2.49–2.56 (1H, m, CH), 2.27–2.36 (1H, m, CH), 2.00–2.15 (1H, m, CH), 1.81–1.94 (2H, m, 2× CH),1.54–1.79 (6H, m, 6× CH), 1.00–1.25 (5H, m, 5× CH); δ_C ($CDCl_3$) 179.8, 163.8, 158.7, 136.6, 128.4, 128.3, 128.0, 67.0, 64.5, 62.4, 51.1, 31.6, 31.5, 30.8, 25.8, 25.4, 25.4, 24.6; ν_{max} (KBr disk) 3407, 3273, 3058, 2932, 1702, 1650, 1604, 1450, 1374, 1090 cm^{-1}; MS (ESI) *m*/*z* 373.2 (100%, $[M + H]^+$), HRMS (ESI) *m*/*z* found 373.2233, $C_{20}H_{29}N_4O_3^+$ ($[M + H]^+$) requires 373.2234.

(*S*)-*N*-(*N*,*N*′-Diphenylcarbamimidoyl)-1-methylpyrrolidine-2-carboxamide 26a: method A. *N*-Methyl-L-proline **23a** (2.0 g, 15.5 mmol, 1.0 equiv.); dry DMF (8 mL); CDI (3.01 g, 18.6 mmol, 1.2 equiv.); 24 h; *N*,*N*′-diphenylguanidine (3.27 g, 15.5 mmol, 1.0 equiv.); 24 h. Extraction and column chromatography (0–80% EA in PE) gave **26a** (1.37 g, 4.25 mmol) in 28% as a yellow solid. R_f 0.39 (80% EA in PE); mp 110 °C; $[\alpha]_D^{20}$ +38.1 ($CHCl_3$, $c = 1.0$); δ_H (D_6-DMSO) 9.92 (1H, br s, NH), 9.78 (1H, s, NH), 7.70 (2H, d, *J* 7.8 Hz, 2× CH), 7.29–7.34 (4H, m, 4× CH), 6.99–7.07 (2H, m, 2× CH), 6.90 (2H, d, *J* 7.6 Hz, 2× CH), 2.93 (1H, dd, *J* 4.1, 10.5 Hz, CH), 2.65 (1H, br t, 7.6 Hz, CH), 2.20 (1H, ddd, *J* 6.1, 9.1, 10.5 Hz, CH). 2.10 (3H, s, Me), 2.02–2.14 (1H, m, CH), 1.61–1.77 (2H, m, 2× CH), 1.36–1.51 (1H, m, CH); δ_C (D_6-DMSO) 174.3, 147.4, 140.8, 139.2, 129.2, 128.7, 122.7, 122.4, 122.2, 119.3, 68.1, 55.7, 40.8, 30.3, 24.2; ν_{max} (KBr disc) 3550, 3057, 2944, 1701, 1604, 1420, 1321, 1208, 1157, 1080 cm^{-1}; MS (ESI) *m*/*z* 323.2 (100%, $[M + H]^+$); HRMS (ESI) *m*/*z* found 323.1865, $C_{19}H_{23}N_4O^+$ ($[M + H]^+$) requires 323.1866.

(*S*)-1-Benzyl-*N*-(*N*,*N*′-diphenylcarbamimidoyl)pyrrolidine-2-carboxamide 26b: method A. *N*-Benzyl-L-proline **23b** (1.0 g, 4.87 mmol, 1.0 equiv.); DMF (4 mL); CDI (0.95 g, 5.85 mmol, 1.2 equiv.); 5 h; *N*,*N*′-diphenylguanidine (1.03 g, 4.87 mmol, 1.0 equiv.); 24 h. Extraction, co-evaporation with toluene and column chromatography (0–60% EA in PE) gave **26b** (0.64 g, 1.60 mmol) in 33% yield as a pale yellow solid. R_f 0.32 (30% EA in PE); mp 135–136 °C; $[\alpha]_D^{21}$ +22.3 ($CHCl_3$, $c = 1.0$); δ_H (D_6-DMSO) 9.97 (1H, s, NH), 9.89 (1H, s, NH), 7.67 (2H, d, *J* 7.6 Hz, 2× CH), 7.38 (2H, t, *J* 7.7 Hz, 2× CH), 7.30 (2H, t, *J* 7.8 Hz, 2× CH) 7.17–7.23 (3H, m, 3× CH), 7.10 (1H, t, *J* 7.3 Hz, CH) 7.01 (1H, t, *J* 7.4 Hz, CH), 6.98 (2H, d, *J* 7.7 Hz, 2× CH), 6.69–6.75 (2H, m, 2× CH), 3.66 (1H, d, *J* 13.0 Hz, CH), 3.37 (1H, d, *J* 13.0 Hz, CH), 3.27 (1H, dd, *J* 3.5, 10.2 Hz, CH), 2.59–2.66 (1H, m, CH), 2.09–2.28 (2H, m, 2× CH), 1.82–1.92 (1H, m, CH), 1.68–1.78 (1H, m, CH), 1.51–1.64 (1H, m, CH); δ_C (D_6-DMSO) 174.8, 147.0, 140.3, 139.0, 137.7, 129.4, 128.7, 128.3, 128.3, 127.0, 122.8, 122.4, 122.3, 119.3, 66.7, 58.7, 53.3, 30.2, 24.0; ν_{max} (KBr disc) 3550, 3054, 2924, 1698, 1651, 1588, 1321, 1205, 1077, 1028 cm^{-1}; MS (ESI) *m*/*z* 399.2 (100%, $[M + H]^+$); HRMS (ESI) *m*/*z* found 399.2177, $C_{25}H_{27}N_4O^+$ ($[M + H]^+$) requires 399.2179.

(*S*)-*N*-(*N*,*N*′-Diphenylcarbamimidoyl)-1-isopropylpyrrolidine-2-carboxamide 26c: method A. *N*-Isopropyl-L-proline **23c** (1.0 g, 6.36 mmol, 1.0 equiv.); DMF (10 mL); (1.24 g, 7.63 mmol, 1.2 equiv.); 5 h; *N*,*N*′-diphenylguanidine (1.30 g, 6.36 mmol, 1.0 equiv.); 16 h. Extraction and column chromatography (0–80% EA in PE) gave **26c** (1.87 g, 5.34 mmol) in 84% yield as a pale yellow solid. R_f 0.32 (20% EA/PE); mp 136 °C; $[\alpha]_D^{16}$ +52.1 ($CHCl_3$, $c = 1.0$); δ_H ($CDCl_3$) 10.23 (1H, s, NH), 9.98 (1H, s, NH), 7.73 (2H, d, *J* 7.9 Hz, 2× CH), 7.27–7.37 (4H, m, 4× CH), 6.99–7.08 (2H, m, 2× CH), 6.94 (2H, d, *J* 7.7 Hz, 2× CH), 3.25 (1H, dd, *J* 1.8, 9.6 Hz, CH), 2.68 (1H, br t, *J* 7.4 Hz, CH), 2.47–2.56 (1H, m, CH), 2.29–2.38 (1H, m, CH), 1.92–2.08 (2H, m, 2× CH), 1.68–1.77 (1H, m, CH), 1.46–1.58 (1H, m, CH), 0.74 (6H, d, *J* 5.1 Hz, 2× Me); δ_C ($CDCl_3$) 176.4, 147.7, 140.9, 139.2, 129.5, 128.8, 123.0, 122.6, 122.5, 119.7, 64.7, 52.8, 50.2, 31.4, 24.7, 21.4, 19.6; ν_{max} (KBr disk) 3350, 3261, 3050, 2829, 1791, 1680, 1588, 1301, 1079, 894 cm^{-1}; MS (EI) *m*/*z* 349.2 (3%, $[M - H]^-$); MS (ESI) *m*/*z* 351.2 (100%, $[M + H]^+$); HRMS (ESI) *m*/*z* found 351.2183, $C_{21}H_{27}N_4O^+$ ($[M + H]^+$) requires 351.2179.

(*S*)-1-Cyclohexyl-*N*-(*N*,*N*′-diphenylcarbamimidoyl)pyrrolidine-2-carboxamide 26d: method A. *N*-Cyclohexyl-L-proline **26d** (1.01 g, 5.07 mmol, 1.0 equiv.) DMF (5 mL); CDI (0.99 g, 6.08 mmol, 1.2 equiv.); 4 h; *N*,*N*′-diphenylguanidine (1.07 g, 5.07 mmol, 1.0 equiv.); 18 h. Extraction and trituration with DE (2× 50 mL) gave **26d** (1.67 g, 4.28 mmol) in 84% yield as an off white solid. R_f 0.25 (15% EA/PE); mp 78–79 °C; $[\alpha]_D^{15}$ +6.5 (MeOH, $c = 1.0$); δ_H ($CDCl_3$) 10.23 (1H, s, NH), 10.02 (1H, s, NH), 7.74 (2H, d, *J* 7.9 Hz, 2× CH), 7.30–7.35 (4H, m, 4× CH), 7.06 (1H, t, *J* 7.4 Hz, CH), 7.03 (1H, t, *J* 7.4 Hz, CH), 6.94 (2H, d, *J* 7.8 Hz, 2× CH), 3.28 (1H, dd, *J* 3.0, 9.5 Hz, CH), 2.72 (1H, dd, *J* 7.5, 7.7 Hz, CH), 2.33 (1H, ddd, *J* 5.6, 9.0, 11.4, CH), 2.05–2.13 (1H, m, CH), 1.93–2.05 (2H, m, 2× CH), 1.68–1.75 (1H, m, CH) 1.53–1.67 (4H, m, 6× CH), 1.42–1.52 (1H, m, CH), 1.33–1.40 (1H, m, CH), 0.93–1.15 (3H, m, 3× CH), 0.81 (1H, dq, *J* 3.3, 12.4 Hz, CH), 0.67 (1H, dq, *J* 3.5, 12.4 Hz, CH); δ_C ($CDCl_3$) 176.5, 147.8, 140.9, 139.2, 129.5, 128.8, 123.0, 122.6, 122.6, 119.7, 64.5, 61.6, 50.5, 31.9, 31.2, 30.1, 25.8, 25.2, 25.1, 24.6; ν_{max} (KBr disk) 3058, 2927, 1691, 1650, 1589, 1316, 1028, 750 cm^{-1}; MS (ESI) *m*/*z* 391.2 (%, $[M + H]^+$); HRMS (ESI) *m*/*z* found 391.2482; $C_{24}H_{31}N_4O^+$ $[M + H]^+$ requires 391.2492.

(*S*)-1-Methyl-*N*-(*N*′-phenylcarbamimidoyl)pyrrolidine-2-carboxamide 27a: method B. *N*-Methyl-L-proline **23a** (0.50 g, 3.87 mmol, 1.0 equiv.); DMF (10 mL); CDI (0.75 g, 4.65 mmol, 1.2 equiv.); 3 h; Na (0.09 g, 3.87 mmol, 1.0 equiv.); methanol (4 mL) 2-phenylguanidinium nitrate (0.84 g, 4.26 mmol, 1.1 equiv.); 5 d. Extraction and column chromatography (0–50% EA in PE) gave **27a** (0.38 g, 1.53 mmol) in 40% yield as a pale yellow solid. R_f 0.28 (50% EA in PE); mp 133 °C; $[\alpha]_D^{16}$ −80.1 ($CHCl_3$, $c = 1.0$); δ_H ($CDCl_3$) 7.32 (2H, t, *J* 7.8 Hz, 2× CH), 7.06 (1H, t, *J* 7.4H, CH), 6.96–7.00, (2H, m, 2× CH), 5.03–6.85 (3H, br s, 3× NH), 3.12–3.22 (1H, m, CH), 3.02 (1H, dd, *J* 4.8, 10.4 Hz, CH), 2.44 (3H, s, Me), 2.36–2.46 (1H, m, CH), 2.21–2.32 (1H, m, CH), 1.91–2.02 (1H, m, CH), 1.76–1.86 (2H, m, 2× CH); δ_C ($CDCl_3$) 176.7, 148.2, 146.1, 129.7, 123.6, 122.9, 69.2, 56.5, 41.7, 31.1, 24.5; ν_{max} (KBr disc) 3314, 3085, 2903, 1631, 1590, 1515, 1391, 1286, 1183, 1039 cm^{-1}; MS (ESI) *m*/*z* 247.2 (100%, $[M + H]^+$); HRMS (ESI) *m*/*z* found 247.1556, $C_{13}H_{19}N_4O^+$ ($[M + H]^+$) requires 247.1553.

(*S*)-1-Benzyl-*N*-(*N*′-phenylcarbamimidoyl)pyrrolidine-2-carboxamide 27b: method B. *N*-Benzyl-L-proline **23b** (2.0 g, 9.74 mmol, 1.0 equiv.); DMF (10 mL); CDI (1.9 g, 11.69 mmol, 1.20 equiv.); 16 h; Na metal (0.224 g, 9.74 mmol 1.0 equiv.); methanol (8 mL) *N*,*N*′-diphenylguanidine (1.93 g, 9.74 mmol, 1.0 equiv.); 5 d. Extraction and column chromatography (0–50% EA in PE) gave **27b** (1.63 g, 5.06 mmol) in 52% yield as a yellow gum. R_f 0.31 (20% EA/PE); $[\alpha]_D^{16}$ −47.6 ($CHCl_3$, $c = 1.0$); δ_H ($CDCl_3$) 7.24–7.37 (7H, m, 7× CH), 7.08 (1H, t, *J* 7.4 Hz, CH), 6.98 (2H, d, *J* 7.4 Hz, 2× CH), 5.22–9.48 (3H, br s, 3× NH), 3.81 (1H, d, *J* 12.1 Hz, CH), 3.68 (1H, d, *J* 12.1 Hz, CH), 3.27 (1H, dd, *J* 4.4, 10.4 Hz, CH), 3.01–3.18 (1H, m, CH), 2.41–2.52 (1H, m, CH), 2.18–2.33 (1H, m, CH), 1.93–2.03 (1H, m, CH), 1.73–1.86 (2H, m, 2× CH); δ_C ($CDCl_3$) 176.6, 147.4, 147.1, 137.5, 129.6, 129.3, 128.5, 127.5, 123.1, 122.7, 67.2, 59.8, 54.1, 30.9, 24.1; ν_{max} 3413, 3060, 2943, 1659, 1643, 1589, 1305, 1064, 752 cm^{-1}; MS (ESI) *m*/*z* 323.2 (100%, $[M + H]^+$); HRMS (ESI) *m*/*z* found 323.1868, $C_{19}H_{23}N_4O^+$ ($[M + H]^+$) requires 323.1866.

(*S*)-*N*′-Boc-*N*-carbamimidoyl-1-methylpyrrolidine-2-carboxamide 29: method A. *N*-Methyl-L-proline **23a** (2.0 g, 15.5 mmol, 1.0 equiv.); DMF (10 mL); CDI (3.01 g, 18.6 mmol, 1.2 equiv.); 24 h; *N*-Boc-guanidine (2.47 g, 15.48 mmol, 1.0 equiv.); 24 h. Extraction and silica gel chromatography (70–100% EA in PE) gave **29** (1.58 g, 5.85 mmol) as a white solid in 38% yield. R_f 0.3 (5% ME in CF); $[\alpha]_D^{20}$ −46 (CH_2Cl_2, $c = 1.0$); mp 134 °C; δ_H ($CDCl_3$) 8.21–10.03 (3H, br s, NH, NH_2), 3.00–3.07 (1H, m, CH), 2.95 (1H, dd, *J* 10.5, 4.8 Hz, CH), 2.31 (3H, s, CH_3), 2.30–2.38 (1H, m, CH), 2.15–2.26 (1H, m, CH), 1.79–1.89 (1H, m, CH), 1.64–1.97 (2H, m, 2× CH), 1.46 (9H, s, 3× Me); δ_C ($CDCl_3$) 178.0, 163.4, 158.5, 79.4, 69.0, 56.5, 41.7, 31.3, 28.2, 24.6; ν_{max} 3381, 3293, 2974, 2871, 2794, 1704, 1649, 1619, 1430, 1135, 1048 cm^{-1}; MS (ESI) *m*/*z* 171.1 (82%), 271.2 (100%, $[M + H]^+$), 293.2 (13%, $[M + Na]^+$), 563.3 (27%, $[2\,M + Na]^+$); HRMS (ESI) *m*/*z* found 271.1765, $C_{12}H_{23}N_4O_3^+$ ($[M + H]^+$) requires 271.1765.

(*S*)-*N*-(*N*′-Boc-*N*-methylcarbamimidoyl)-1-methylpyrrolidine-2-carboxamide 30: method A. *N*-Methyl-L-proline **23a** (1.12 g, 8.66 mmol, 1.0 equiv.); DMF (12 mL); CDI (2.42 g, 14.94 mmol, 2.0 equiv.); 24 h; *N*-Boc-*N*′-methylguanidine (750.0 mg, 4.33 mmol, 3.45 equiv.); 5 d. Extraction and trituration with DE (2× 50 mL) gave **30** (1.15 g, 4.04 mmol) in 94% yield as off white solid. R_f 0.13 (50% EA in PE); $[\alpha]_D^{18}$ −6.4 (CH_2Cl_2, $c = 1.1$); mp 130–132 °C, δ_H ($CDCl_3$) 12.80 (1H, s, NH), 8.81 (1H, s, NH), 3.21–3.28 (1H, m, CH), 2.99 (1H, dd, *J* 4.6, 9.9 Hz, CH), 2.95 (3H, d, *J* 4.9 Hz, CH_3), 2.41 (3H, s, CH_3), 2.36–2.44 (1H, m, CH), 2.16–2.29 (1H, m, CH), 1.75–1.93 (3H, m, 3× CH), 1.51 (9H, s, 3× Me); δ_C ($CDCl_3$) 177.7, 162.7, 156.0, 79.3, 69.5, 56.5, 41.5, 31.4, 28.4, 27.9, 24.5; ν_{max} 3312, 2975, 1727, 1434, 1152, 1046 cm^{-1}; MS (ESI) *m*/*z* 285.2 (100%, M + H$]^+$), HRMS (ESI) found 285.1919, *m*/*z* $C_{13}H_{25}N_4O_3^+$ ([M + H$]^+$) requires 285.1921.

(*S*)-*N*-(*N*′-Cbz-*N*-methylcarbamimidoyl)-1-methylpyrrolidine-2-carboxamide 31: method A. *N*-Methyl-L-proline **23a** (935.0 mg, 7.24 mmol, 1.5 equiv.); DMF (12 mL); CDI (1.96 g, 12.06 mmol, 2.5 equiv.); 24 h; *N*-methyl-*N*-Cbz-buanidine (1.0 g, 4.83 mmol, 1.0 equiv.); 4 d. Extraction and recrystallization from methanol gave **31** (1.37 g, 4.30 mmol) in 89% yield as a white solid. R_f 0.23 (50% EA/PE); $[\alpha]_D^{20}$ −54.0 (CH_3Cl, $c = 1.1$); mp 100–102 °C, δ_H ($CDCl_3$) 12.81 (1H, s, NH), 8.99 (1H, s, NH), 7.42 (2H, d, *J* 7.0 Hz, 2× CH), 7.28–7.37 (3H, m, 3× CH) 5.16 (2H, s, CH_2), 3.25–3.32 (1H, m, CH), 3.00 (1H, dd, *J* 4.7, 10.0 Hz, CH), 2.97 (3H, d, *J* 4.9 Hz, CH_3), 2.43 (3H, s, CH_3), 2.37–2.43 (1H, m, CH), 2.20–2.32 (1H, m, CH), 1.77–1.94 (3H, m, 3× CH); δ_C ($CDCl_3$) 178.0, 163.0, 156.6, 137.0, 128.5, 128.4, 128.0, 69.6, 67.2, 56.6, 41.6, 31.5, 27.9, 24.5; ν_{max} 3298, 3130, 2946, 2851, 2793, 1691, 1642, 1618, 1562, 1497, 1436, 1124, 1082, 874 cm^{-1}; MS (ESI) *m*/*z* 319.2 (100%, [M + H$]^+$), HRMS (ESI) *m*/*z* found 319.1767, $C_{16}H_{23}N_4O_3^+$ ([M + H$]^+$) requires 319.1765.

(*S*)-*N*-(1*H*-Benzo[*d*]imidazol-2-yl)-1-methylpyrrolidine-2-carboxamide 34a: method A. *N*-Methyl-L-proline **23a** (1.0 g, 7.74 mmol, 1.0 equiv.); DMF (9 mL); CDI (1.51 g, 9.29 mmol, 1.2 equiv.); 4 h; 2-aminobenzimidazole (1.05 g, 7.74 mmol, 1.0 equiv.); 38 h. Extraction and column chromatography (0–50% ME in EA) gave **34a** (1.04 g, 4.25 mmol) in 55% yield as a pale yellow solid. R_f 0.16 (20% ME in EA); mp 242–244 °C; $[\alpha]_D^{16}$ −117 ($CDCl_3$, $c = 1.0$); δ_H ($CDCl_3$) 10.92 (1H, br s, NH), 10.47(1H, br s, NH), 7.24–7.74 (2H, m, 2× CH), 7.06–7.22 (2H, m, 2× CH), 3.01–3.18 (2H, m, 2× CH), 2.39 (3H, s, Me), 2.33–2.45 (1H, m, CH), 2.18–2.32 (1H, m, CH), 1.87–1.99 (1H, m, CH), 1.68–1.83 (2H, m, 2× CH); δ_C ($CDCl_3$) 175.3, 146.3, 138.3, 122.3, 122.3, 68.7, 56.7, 41.9, 31.4, 24.8; ν_{max} (KBr disk) 3350, 3244, 3050, 2946, 1702, 1626, 1589, 1310, 1021, 861 cm^{-1}; MS (ESI) *m*/*z* 267.1 (100%, [M + Na$]^+$), 245.1 (55%, [M + H$]^+$), HRMS (ESI) *m*/*z* found 245.1399, $C_{13}H_{17}N_4O^+$ ([M + H$]^+$) requires 245.1397.

(*S*)-*N*-(1*H*-Benzo[*d*]imidazol-2-yl)-1-benzylpyrrolidine-2-carboxamide 34b: method A. *N*-Benzyl-L-proline **23b** (1.0 g, 4.87 mmol, 1.0 equiv.); DMF (9 mL); CDI (0.95 g, 5.85 mmol, 1.2 equiv.); 4 h; 2-aminobenzimidazole (0.69 g, 4.87 mmol, 1.0 equiv.); 48 h. Extraction and column chromatography (0–100% EA in PE) gave **34b** (1.48 g, 4.64 mmol) in 96% as a pale yellow solid. R_f 0.47 (20% EA in PE); mp 228–229 °C; $[\alpha]_D^{16}$ −106.8 ($CDCl_3$, $c = 1.0$); δ_H ($CDCl_3$) 10.89 (1H, br s, NH), 10.37 (1H, br s, NH), 7.53–7.71 (1H, m, CH), 7.15–7.42 (8H, m, 8× CH), 3.86 (1H, d, *J* 12.7 Hz, CH), 3.72 (1H, d, *J* 12.7 Hz, CH), 3.43 (1H, dd, *J* 10.6, 4.2 Hz, CH), 3.15 (1H, t, *J* 7.4, CH), 2.49–2.58 (1H, m, CH), 2.24–2.39 (1H, m, CH), 1.97–2.06 (1H, m, CH), 1.73–1.90 (2H, m, CH_2); δ_C ($CDCl_3$) 175.3, 146.1, 137.3, 134.7, 129.3, 128.8, 127.8, 122.3, 122.3, 66.7, 60.1, 54.3, 31.1, 24.5; ν_{max} (KBr disk) 3350, 3253, 3025, 2942, 1768, 1688, 1624, 1307, 1047, 744 cm^{-1}; MS (ESI) *m*/*z* 321.2 (100%, [M + H$]^+$); HRMS (ESI) *m*/*z* found 321.1710, $C_{19}H_{21}N_4O^+$ ([M + H$]^+$) requires 321.1710.

(*S*)-*N*-(1*H*-Benzo[*d*]imidazol-2-yl)-1-isopropylpyrrolidine-2-carboxamide 34c: method A. *N*-Isopropyl-L-proline **23c** (1.0 g, 6.36 mmol, 1.0 equiv.); DMF (10 mL); CDI (1.25 g, 7.63 mmol, 1.2 equiv.); 3 h; 2-aminobenzimidazole (0.86 g, 6.36 mmol, 1.0 equiv.); 40 h. Extraction and column chromatography (0–100% EA in PE) gave **34c** (1.48 g, 5.45 mmol) in 86% as a pale yellow solid. R_f 0.25 (20% EA in PE); mp 112–114 °C; $[\alpha]_D^{16}$ −110.5 ($CHCl_3$, $c = 1.0$); δ_H ($CDCl_3$) 11.05 (1H, br s, NH), 10.65 (1H, br s, NH), 7.34–7.81 (2H, m, 2× CH), 7.19–7.247 (2H, m, 2× CH), 3.50 (1H, dd, *J* 2.7, 10.5 Hz, CH), 3.20 (1H, br t, *J* 7.6 Hz, CH), 2.87 (1H, septet, *J* 6.4 Hz, CH), 2.61 (1H, ddd, *J* 5.9, 9.3, 10.9, CH), 2.13–2.24 (1H, m, CH), 2.02–2.11 (1H, m, CH), 1.69–1.89 (2H, m, CH_2), 1.13 (3H, d, *J* 6.4 Hz, Me), 1.12 (3H, d, *J* 6.4 Hz, Me); δ_C ($CDCl_3$) 176.7, 146.1, 122.3, 122.3, 64.2, 53.4, 50.9, 31.7, 24.9, 21.5, 20.1 (1× C not observed); ν_{max} (KBr disk) 3312, 3071, 2927, 1680, 1610, 1553, 1304, 1095, 747 cm^{-1}; MS (ESI) *m*/*z* 273.2 (100%, [M + H$]^+$), HRMS (ESI) *m*/*z* found 273.1710, $C_{15}H_{21}N_4O^+$ ([M + H$]^+$) requires 273.1710.

(*S*)-*N*-(1*H*-Benzo[*d*]imidazol-2-yl)-1-cyclohexylpyrrolidine-2-carboxamide 34d: method A. *N*-Cyclohexyl-L-proline **23d** (1.0 g, 5.07 mmol, 1.0 equiv.); DMF (10 mL); CDI (0.99 g, 6.08 mmol, 1.2 equiv.); 4 h; 2-aminobenzimidazole (0.71 g, 5.07 mmol, 1.0 equiv.); 48 h. Extraction and column chromatography (0–60% EA in PE) gave **34d** (1.32 g, 4.23 mmol) in 84% as a pale yellow solid. R_f 0.37 (20% EA in PE); mp 129–130 °C; $[\alpha]_D^{15}$ −105.1 (ME, $c = 1.0$); δ_H ($CDCl_3$) 8.40–12.50 (2H, br s, 2× NH) 7.36–7.67 (2H, br m, 2× CH), 7.22–7.27 (2H, m, 2× CH), 3.55 (1H, dd, *J* 2.6, 10.6 Hz, CH), 3.23 (1H, br t, *J* 7.4 Hz, CH), 2.63 (1H, ddd, *J* 5.7, 8.1, 11.1, CH), 2.39–2.50 (1H, m, CH), 2.13–2.24 (1H, m, CH), 2.04–2.11 (1H, m, CH), 1.94–2.02 (1H, m, CH), 1.69–1.90 (5H, m, 5× CH), 1.64 (1H, br d, *J* 11.1 Hz, CH), 1.18–1.33 (1H, m, 4× CH), 1.05–1.18 (1H, m, CH); δ_C (CD_3OD) 175.5, 147.1, 138.6, 123.2, 123.2, 65.4, 63.6, 52.1, 33.1, 32.2, 31.9, 27.0, 26.5, 26.4, 25.5; ν_{max} (KBr disk) 3309, 3230, 3056, 2927, 1686, 1627, 1589, 1308, 1029, 743 cm^{-1}; MS (ESI) *m*/*z* 313.2 (100%, [M + H$]^+$); HRMS (ESI) *m*/*z* found 313.2016, $C_{18}H_{25}N_4O^+$ [M + H$]^+$ requires 313.2023.

(*S*)-*N*-(1*H*-Benzo[*d*]imidazol-2-yl)-1-methylpyrrolidine-2-carboxamide 35: method A. *N*-Methyl-L-proline **23a** (658.2 mg, 5.10 mmol, 1.50 equiv.); DMF (12 mL); CDI (1.38 g, 8.49 mmol, 2.5 equiv.); 8 h; 1-methyl-2-aminobenzimidazole (0.50 g, 3.40 mmol, 1.0 equiv.); 10 d. Extraction and silica gel chromatography, eluting with (2.5–6% ME in CF), gave **35** (357.0 mg, 0.138 mmol) in 41% yield as a tan coloured gum. R_f 0.24 (50% $CHCl_3$/MeOH); $[\alpha]_D^{23}$ −32.2 (CH_2Cl_2, $c = 1.6$); δ_H ($CDCl_3$) 9.40–11.24 (1H, br s, NH), 7.53 (1H, br d, *J* 6.0 Hz, CH), 7.22–7.30 (3H, m, 3× CH), 3.69 (3H, s, CH_3), 3.26 (1H, br t, *J* 7.5 Hz, CH), 3.10–

3.18 (1H, m, CH), 2.54 (3H, s, CH_3), 2.40–2.51 (1H, m, CH), 2.25–2.36 (1H, m, CH), 2.02–2.12 (1H, m, CH), 1.81–2.00 (2H, m, 2× CH); δ_C ($CDCl_3$) 175.1 (HMBC), 155.4 (HMBC), 135.5 (HMBC), 122.7, 109.3, 70.2, 56.9, 41.8, 31.1, 30.1, 24.2; ν_{max} 3342, 2981, 2922, 2851, 1626, 1557, 1483, 1454, 1065 cm^{-1}; MS (ESI) *m*/*z* 259.2 (100%, $[M + H]^+$), 539.3 (64%, $[2 M + Na]^+$), 281.1 (59%, $[M + Na]^+$); HRMS (ESI) *m*/*z* found 259.1555; $C_{14}H_{18}N_4O^+$ ($[M + H]^+$) requires 259.1553.

(*S*)-*N*-(1*H*-Benzo[*d*]imidazol-2-yl)-*N*,1-dimethylpyrrolidine-2-carboxamide 36: method A. *N*-Methyl-L-proline **23a** (1.32 g, 10.19 mmol, 1.5 equiv.); DMF (11 mL); CDI (2.75 g, 16.99 mmol, 2.5 equiv.); 8 h; *N*-methyl-1*H*-benzo[*d*]imidazol-2-amine (1.0 g, 6.79 mmol, 1.0 equiv.); 3 d. Extraction and recrystallization (DE/PE) gave **36** (970.0 mg, 3.06 mmol) in 45% yield as an off-white solid. R_f 0.13 (3% MeOH in $CHCl_3$); mp 112–114 °C; $[\alpha]_D^{18}$ −84.4 (CH_2Cl_2, $c = 1.3$); δ_H ($CDCl_3$) 11.60 (1H, s, NH), 7.64 (1H, d, *J* 5.8 Hz, CH), 7.39 (1H, d, *J* 5.8 Hz, CH), 7.16–7.25 (2H, m, 2× CH), 3.78 (3H, s, CH_3), 3.39 (1H, dd, *J* 7.2, 8.6 Hz, CH), 3.22–3.29 (1H, m, CH), 2.44 (3H, s, CH_3), 2.25–2.47 (2H, m, 2× CH), 1.82–2.08 (3H, m, 3× CH); δ_C ($CDCl_3$) 174.9 (HMBC), 149.9, 122.3, 118.3, 110.8, 68.0, 56.2, 41.0, 33.9, 29.7, 23.4; ν_{max} 3361, 3055, 2948, 2850, 2786, 1672, 1622, 1525, 1427, 1308 cm^{-1}; MS (ESI) *m*/*z* 259.2 (100%, $[M + H]^+$) 539.3 (16%, $[2 M + Na]^+$), 281.1 (9%, $[M + Na]^+$) HRMS (ESI) *m*/*z* found 259.1555, $C_{13}H_{19}N_4O^+$ ($[M + H]^+$) requires 259.1553.

(*S*)-*N*-(Benzo[*d*]thiazol-2-yl)-1-methylpyrrolidine-2-carboxamide 37a: method A. (*S*)-1-Methylpyrrolidine-2-carboxylic acid **23a** (1.00 g, 7.74 mmol, 1.6 equiv.); CDI (2.93 g, 3.5 equiv.); DMF (10 mL); 16 h; 2-aminobenzothiazole (786.0 mg, 1.0 equiv.); 7 d. Extraction and column chromatography (0–50% EA in PE with 0.1% NH_3) gave **37a** (1.00 g, 3.81 mmol, 74%) as a white solid. R_f 0.10 (30% EA in PE with 0.1% NH_3); mp 79–83 °C, $[\alpha]_D^{19}$ −38.0 ($CHCl_3$, $c = 1.0$); δ_H ($CDCl_3$) 9.82–11.72 (1H, br s, NH), 7.82 (1H, d, *J* 7.9 Hz, CH), 7.78 (1H, d, *J* 8.1 Hz, CH), 7.44 (1H, dd (apparent t), *J* 7.5, 8.1 Hz, CH), 7.31 (1H, dd (apparent t), *J* 7.5, 7.9 Hz, CH), 3.17–3.30 (2H, m, 2× CH), 2.49 (3H, s, CH_3), 2.44–2.55 (1H, m, CH), 2.26–2.40 (1H, m, CH), 1.97–2.07 ((1H, m, CH), 1.76–1.92 (2H, m, CH_2); δ_C ($CDCl_3$) 173.7, 157.7, 148.6, 132.3, 126.4, 124.1, 121.6, 121.1, 68.5, 56.7, 42.0, 31.3, 24.9; ν_{max} 3182, 2949, 2848, 2796, 1696, 1600, 1628, 1445, 1352, 1316, 1263, 1156, 1048, 1016, 779, 757, 730, 668 cm^{-1}; MS (ESI) *m*/*z* 284.1 (100%, $[M + Na]^+$), 262.1 (95%, $[M + H]^+$), 545.2 (42%, $[2M + Na]^+$); HRMS (ESI) *m*/*z* found 262.1011, $C_{13}H_{15}N_4OS^+$ ($[M + H]^+$) requires 262.1009.

(*S*)-1-Methyl-*N*-(1*H*-imidazol-2-yl)pyrrolidine-2-carboxamide 38a: method A. *N*-Methyl-L-proline **175a** (1.00 g, 7.74 mmol, 1.0 equiv.); CDI (2.26 g, 13.94 mmol, 1.8 equiv.); DMF (15 mL); 24 h; 2-aminoimidazole hemisulfate (1.26 g, 9.54 mmol, 1.23 equiv.); Et_3N (3.04 mL, 34.8 mmol, 4.5 equiv); 24 h. Extraction and column chromatography (5–80% EA in PE with 0.1% NH_3) gave **270** (1.47 g, 7.57 mmol, 97%) as a off-white solid. R_f 0.24 (10% EA in ME); mp 180–182 °C; $[\alpha]_D$ −73.3 ($c = 0.3$, $CHCl_3$); δ_H ($CDCl_3$) 9.55–11.41 (2H, br s, 2× NH), 6.82 (2H, s, 2× CH), 3.15–3.19 (1H, m, CH), 3.08 (1H, dd, *J* 4.6, 10.5 Hz, CH), 2.44 (3H, s, Me) 2.40–2.47 (1H, m, CH) 2.23–2.33 (1H, m, CH) 1.91–1.98 (1H, m, CH), 1.74–1.86 (2H, m, CH_2); δ_C ($CDCl_3$) 174.3, 140.5, 68.5, 56.8, 42.0, 31.4, 24.8 (imidazole 2× CH not detected); ν_{max} 3223, 2960, 2845, 2786, 1671, 1585, 1524, 1492 cm^{-1}; MS (ESI) *m*/*z* 195.1 (100%, $[M + H]^+$); HRMS (ESI) *m*/*z* found 195.1240, $C_9H_{15}N_4O$ ($[M + H]^+$) requires 195.1241.

(*S*)-1-Benzyl-*N*-(1*H*-imidazol-2-yl)pyrrolidine-2-carboxamide 38b: method A. *N*-Benzyl-L-proline **23b** (1.00 g, 4.87 mmol, 1.0 equiv.); CDI (1.44 g, 8.77 mmol, 1.80 equiv.); DMF (15 mL); 16 h; 2-aminoimidazole hemisulfate (0.772 g, 5.84 mmol, 1.2 equiv.); Et_3N (2.21 g, 21.9 mmols, 3.04 mL, 4.5 equiv.); 2 d. Extraction and column chromatography (5–80% EA in PE) gave **38b** (0.897 g, 3.32 mmol) in 68% yield as a white solid. R_f 0.31 (50% EA in PE); mp 64 °C; $[\alpha]_D$ −198 ($c = 1$, $CHCl_3$); δ_H ($CDCl_3$) 9.38–11.51 (2H, br m, 2× NH), 7.15–7.31 (5H, m, Ph), 6.76 (2H, s, 2× CH), 3.82 (1H, d, *J* 12.7 Hz, CH), 3.57 (1H, d, *J* 12.7 Hz, CH), 3.31 (1H, dd, *J* 4.2, 10.4 Hz, CH), 3.00–3.07 (1H, m, CH), 2.37–2.46 (1H, m, CH), 2.16–2.27 (1H, m, CH), 1.87–1.97 (1H, m, CH), 1.66–1.82 (2H, m, 2× CH); 174.1, 141.3, 137.6, 129.2, 128.7, 127.6, 66.7, 60.0, 54.0, 30.9, 24.3 (imidazole 2× CH not detected); ν_{max} 3269, 3025, 2973, 29 251, 2804, 1665, 1571, 1525, 1493 cm^{-1}; MS (CI) *m*/*z* 160.1 (100%), 269.1 (40%, $[M - H]^+$) 293.1 (55% $[M + Na]^+$); HRMS (CI) *m*/*z* found 293.1376, $C_{15}H_{18}N_4ONa$ ($[M + Na]^+$) requires 293.1373.

(*S*)-1-Methyl-*N*-(pyridine-2-yl)pyrrolidine-2-carboxamide 39a: method A. *N*-Methyl-L-proline **23a** (1.00 g, 7.74 mmol, 1.5 equiv.); CDI (2.93 g, 3.5 equiv.); DMF (10 mL); 16 h; 2-aminopyridine (486.0 mg, 5.16 mmol, 1.0 equiv.); 7 d. Extraction, column chromatography (0–50% EA in PE with 0.1% NH_3) and recrystallization (CF) gave **39a** (189.6 mg, 0.92 mmol) in 18% yield as pale yellow-green crystals. R_f 0.26 (15% EA in PE); mp 40–41 °C; $[\alpha]_D^{20}$ −78.9 ($c = 1.0$ in CF); δ_H ($CDCl_3$) 9.85 (1H, s, NH), 8.29 (H, br d, *J* 4.7 Hz, CH), 8.26 (1H, br d, *J* 8.4 Hz, CH), 7.69 (1H, ddd, *J* 1.6, 7.2, 8.4 Hz, CH), 7.02 (1H, t, *J* 4.7, 7.2 Hz, CH), 3.17–3.22 (1H, m, CH), 2.99–3.10 (1H, m, CH), 2.46 (3H, s, Me), 2.39–2.46 (1H, m, CH), 2.24–2.35 (1H, m, CH), 1.92–2.02 (1H, m, CH_2), 1.77–1.88 (2H, m, CH_2); δ_C 178.4, 151.4, 148.1, 138.4, 119.8, 113.9, 69.5, 56.7, 41.9, 31.3, 24.6; ν_{max} 3301, 2950, 2850, 2711, 1705, 1570, 1508, 1433, 1271, 765 cm^{-1}; MS (CI) *m*/*z* 228.1 (100%, [M + Na]), 206.1 (20%, $[M + H]^+$); HRMS (CI) *m*/*z* found 206.1289, $C_{11}H_{16}N_3ONa$ ($[M + H]^+$) requires 206.1288.

(2*S*,2′*S*)-*N*,*N*′-(Iminomethylene)bis(1-benzylpyrrolidine-2-carboxamide) 40b: method C. *N*-Benzyl-L-proline **23b** (2.0 g, 9.74 mmol, 1.0 equiv.); CDI (1.92 g, 11.7 mmol, 1.2 equiv.); DMF (6 mL); 16 h; NaH (60%, 0.234 g, 5.85 mmol, 0.60 equiv.); DMF (10 mL); guanidinium chloride (0.97 g, 4.87 mmol, 0.50 equiv.); 48 h. Extraction and column chromatography (25–27% EA in PE) gave **40b** (1.66 g, 3.84 mmol) as an off-white solid in 79% yield. R_f 0.25 (30% EA in PE); mp 125–127 °C; $[\alpha]_D^{19}$ −83.3 (CH_2Cl_2, $c = 1.2$); δ_H ($CDCl_3$) 8.17–11.43 (3H, br s, 3× NH), 7.19–7.39 (10H, m, 2× Ph) 3.86 (2H, d, *J* 12.8 Hz, 2× CH), 3.61 (2H, d, *J* 12.7 Hz, 2× CH), 3.22 (2H, dd, *J*, 5.9, 9.7 Hz, 2× CH), 3.11–3.15 (2H, m, 2× CH), 2.38–2.44 (2H, m, 2× CH), 2.17–2.28 (2H, m, 2× CH), 1.91–2.02 (2H, m, 2× CH), 1.76–1.90 (4H, m, 2× CH_2); δ_C ($CDCl_3$) 176.0, 147.8, 137.8, 129.5, 128.4, 127.4, 68.7, 59.5, 53.9, 30.6, 23.8; ν_{max} 3354, 3027, 2964, 2875, 2805, 1701, 1604, 1494, 1260; MS (ESI) *m*/*z* 434.3 (100%, $[M + H]^+$), 160.1 (72%); HRMS (ESI) found 434.2540, $C_{25}H_{31}N_5O_2^+$ ($[M + H]^+$) requires 434.2551.

(2*S*,2′*S*)-*N*,*N*′-(Iminomethylene)bis(1-isopropylpyrrolidine-2-carboxamide) 40c: method C. *N*-Isopropyl-L-proline **23c** (1.0 g, 6.36 mmol, 1.0 equiv); DMF (5 mL); CDI (1.24 g, 7.36 mmol, 1.2

equiv); 24 h; guanidine hydrochloride (303.8 mg, 3.18 mmol, 0.5 equiv); DMF (10 mL); NaH (60%, 0.38 g, 9.54 mmol, 1.0 equiv.); 48 h. Extraction and column chromatography (50–100% EA in PE) gave **40c** (1.07 g, 3.17 mmol) in 93% yield as an off-white solid. R_f 0.13 (100% EA); mp 121–123 °C; $[\alpha]_D^{23}$ −129.7 (CH_2Cl_2, $c = 1.2$); δ_H ($CDCl_3$) 10.22–12.70 (1H, br s, NH), 8.05–10.22 (2H, br s, 2× NH), 3.25–3.28 (1H, m, CH), 3.04–3.16 (2H, m, 2× CH), 2.70–2.80 (2H, m, 2× CH), 2.46–2.52 (2H, m, 2× CH), 2.00–2.10 (2H, m, 2× CH), 1.83–1.94 (2H, m, 2× CH), 1.64–1.77 (4H, m, 2× CH_2), 1.01 (12H, d, J 6.4 Hz, CH_3); δ_C ($CDCl_3$) 177.3, 148.3, 94.5, 64.9, 53.0, 50.5, 31.8, 24.9, 21.2, 19.9; ν_{max} 3365, 2967, 2874, 1698, 1636, 1611, 1555, 1497, 1308, 1145 cm^{-1}; MS (ESI) m/z 338.3 ($[M + H]^+$); HRMS (ESI) m/z found 338.2553, $C_{17}H_{31}N_5O_2^+$ ($[M + H]^+$) requires 338.2551.

(2*S*,2′*S*)-*N*,*N*′-(Iminomethylene)bis(1-cyclohexylpyrrolidine-2-carboxamide) 40d: method C. *N*-Cyclohexyl-L-proline **23d** (3.0 g, 15.21 mmol, 1.0 equiv.); CDI (2.96 g, 18.25 mmol, 1.20 equiv.); DMF (6 mL) 1 h; NaH (60%, 0.36 g, 9.12 mmol, 0.60 equiv.) DMF (10 mL); guanidinium chloride (0.73 g, 7.60 mmol, 0.50 equiv.) 24 h. Extraction and column chromatography (50–100% EA in PE) gave **40d** (0.50 g, 16% yield, together with 1.87 g, *ca.* 46% yield (*ca.* 95% pure)) as pale yellow crystals. R_f 0.30 (5% ME in EA); mp 157–159 °C; $[\alpha]_D^{17}$ −53.9 (CH_2Cl_2, $c = 1.0$); δ_H ($CDCl_3$) 10.44–12.71 (1H, br s, NH), 8.26–10.44 (2H, br s, 2× NH), 3.37 (2H, dd, J 3.2, 10.3 Hz, 2× CH), 3.15–3.25 (2H, m, 2× CH), 2.52–2.62 (2H, m, 2× CH), 2.32–2.45 (2H, m, 2× CH) 2.04–2.17 (2H, m, 2× CH), 1.87–1.98 (4H, m, 4× CH), 1.69–1.85 (10H, m, 10× CH), 1.61 (2H, br d, J 12.1 Hz, 2× CH), 1.03–1.31 (10H, m, 10× CH); δ_C ($CDCl_3$) 177.2, 150.6, 65.3, 62.0, 50.8, 31.7, 31.5, 30.6, 26.1, 25.6, 25.5, 24.5; ν_{max} 3348, 2965, 2926, 2851, 1693, 1660, 1605, 1462, 108; MS (ESI) m/z 418.3 (100%, $[M + H]^+$), 152.2 (49%); HRMS (ESI) m/z found 418.3168, $C_{23}H_{39}N_5O_2$ ($[M + H]^+$), requires 418.3177.

(*S*)-1-Methylpyrrolidine-2-carbohydrazide 41a: method D. R_f 0.24 (5% ME in CF with 1% NEt_3); $[\alpha]_D^{20}$ −121.6 (CH_2Cl_2, $c = 1.28$); δ_H ($CDCl_3$) 8.25 (1H, br s, NH), 3.74 (2H, br s, NH_2), 3.04 (1H, ddd, J 2.2, 6.5, 8.5 Hz, CH), 2.93 (1H, dd, J 5.1, 10.3 Hz, CH), 2.32 (3H, s, CH_3), 2.25–2.32 (1H, m, CH), 2.12–2.22 (1H, m, CH), 1.66–1.84 (3H, m, CH, CH_2); δ_C ($CDCl_3$) 174.6, 68.1, 56.7, 41.9, 30.9, 24.4; ν_{max} 3297, 2967, 2884, 2785, 1650, 1464, 1085 cm^{-1}; MS (ESI) m/z 144.1 (51%, $[M + H]^+$); HRMS (ESI) m/z found 144.1128, $C_6H_{14}N_3O^+$ ($[M + H]^+$) requires 144.1131.

(*S*)-1-Methyl-*N*′-phenylpyrrolidine-2-carbohydrazide 41b: method A. *N*-Methyl-L-proline **23a** (1.79 g, 13.87 mmol, 1.5 equiv.); DMF (12 mL); CDI (3.75 g, 23.1 mmol, 2.5 equiv.); 24 h; phenyl hydrazine (1.0 g, 9.25 mmol, 1.38 mL, 1.0 equiv.) 2 d. Extraction and column chromatography (3–5% ME in $CHCl_3$), gave **41b** (1.0 g, 4.56 mmol) as a yellow solid in 50% yield. R_f 0.25 (5% ME in EA), $[\alpha]_D^{20}$ −64.6 (CH_3Cl, $c = 1.05$); mp 101–103 °C; δ_H ($CDCl_3$) 8.90 (1H, s, NH), 7.21 (2H, d, J 7.6 Hz, CH), 6.89 (1H, t, J 7.3 Hz, CH), 6.81 (2H, d, J 8.0 Hz, CH), 6.15 (1H, s, NH), 3.14 (1H, m, CH_2), 3.07 (1H, dd, J 10.2, 4.8 Hz,CH_2), 2.47 (3H, s, CH_3), 2.38 (1H, m, CH), 2.33–2.19 (1H, m, CH), 1.98–1.76 (3H, m, CH + CH_2); δ_C ($CDCl_3$) 173.9, 148.2, 129.2, 121.1, 113.6, 68.3, 56.8, 42.2, 31.2, 24.6; ν_{max} 3267, 2965, 2849, 2788, 1672, 1602, 1495, 1351, 1084 cm^{-1}; MS (TOF ASAP) m/z 220.2 (100%, $[M + H]^+$); HRMS (TOF ASAP) m/z found 220.1454, $C_{12}H_{18}N_3O^+$ ($[M + H]^+$) requires 220.1444.

***tert*-Butyl 2-(methyl-L-prolyl)hydrazine-1-carboxylate 41c: method C.** *N*-Methyl-L-proline **23a** (1.47 g, 11.35 mmol, 1.5 equiv.); DMF (15 mL); CDI (3.07 g, 18.92 mmol, 2.5 equiv.); 8 h; *tert*-butyl hydrazine carboxylate (1.02 g, 7.57 mmol, 1.0 equiv.); 3 d. Extraction and recrystallization (ME/CF) gave **41c** (1.1 g, 4.52 mmol) as a white solid in 60% yield. R_f 0.10 (EA); $[\alpha]_D^{20}$ −73.3 (CH_3Cl, $c = 1.08$); mp 102–106 °C; δ_H ($CDCl_3$) 8.74 (1H, br s, NH), 6.47 (1H, br s, NH), 3.05–3.13 (1H, m, CH), 3.00 (1H, dd, J 4.4, 10.2 Hz, CH), 2.42 (3H, s, CH_3), 2.28–2.37 (1H, m, CH), 2.16–2.27 (1H, m, CH), 1.73–1.97 (3H, m, CH, CH_2), 1.47 (9H, s, 3× CH_3); δ_C ($CDCl_3$) 173.7, 155.2, 81.8, 68.3, 56.8, 41.9, 31.0, 28.3, 24.4; ν_{max} 3268, 2967, 2885, 2788, 1726, 1680, 1476, 1391, 1160 cm^{-1}; MS (TOF ASAP) m/z 244.2 (100%, M + H]$^+$); HRMS m/z found 244.1663, $C_{11}H_{22}N_3O_3^+$ ($[M + H]^+$) requires 244.1656.

Benzyl 2-(methyl-L-prolyl)hydrazine-1-carboxylate 41d: method A. *N*-Methyl-L-proline **23a** (1.17 g, 9.03 mmol, 1.5 equiv.); DMF (15 mL); CDI (2.44 g, 15.0 mmol, 2.5 equiv.); 8 h; benzyl hydrazinecarboxylate (1.0 g, 6.02 mmol, 1.0 equiv.); 3 d. Extraction and trituration (DE 3× 50 mL) gave **41d** (1.5 g, 5.41 mmol) as a pale yellow viscous liquid in 90% yield. R_f 0.13 (EA); $[\alpha]_D^{21}$ −61.3 (CH_3Cl, $c = 0.45$); δ_H ($CDCl_3$) 8.82 (1H, s, NH), 7.41–7.29 (5H, m, Ph), 6.75 (1H, s, NH), 5.16 (2H, s, CH_2), 3.15–3.06 (1H, m, CH_2), 3.05–2.95 (1H, m, CH), 2.42 (3H, s, CH_3), 2.34 (1H, m, CH), 2.27–2.13 (1H, m, CH), 2.00–1.87 (1H, m, CH), 1.83–1.67 (2H, m, CH_2); δ_C ($CDCl_3$) 156.1, 135.7, 128.7, 128.5, 128.3, 68.3, 68.0, 56.7, 41.8, 31.0, 24.4; ν_{max} 3265, 2967, 2885, 2791, 1735, 1685, 1466, 1385, 1025 cm^{-1}; MS (ASAP) m/z 278.2 (100%, $[M + H]^+$), 220.2 (58%); HRMS (ASAP) m/z found 278.1505, $C_{14}H_{20}N_3O_3^+$ ($[M + H]^+$) requires 278.1499.

(*S*)-*N*-Cbz-*N*′-carbamimidoyl-2-(dimethylamino)propanamide 43a. Method A. *N*,*N*-Dimethyl-L-alanine **42a** (727.6 mg, 6.21 mmol, 1.2 equiv.); DMF (15 mL); CDI (1.43 g, 8.80 mmol, 1.7 equiv.); 24 h; *N*-Cbz-guanidine (1.0 g, 5.18 mmol, 1.0 equiv.); 4 d. Extraction and column chromatography (30–50% EA in PE) gave **43a** (1.50 g, 5.13 mmol) in 99% yield as a white solid. R_f 0.15 (100% EA); $[\alpha]_D^{23}$ +31.3 (CH_2Cl_2, $c = 1.8$); mp 112–114 °C, δ_H ($CDCl_3$) 8.45–10.94 (3H, br s, 3× NH), 7.23–7.41 (5H, m, CH), 5.11 (2H, s, CH_2), 3.13 (1H, q, J 7.0 Hz, CH), 2.21 (6H, s, 2× CH_3), 1.19 (3H, d, J 7.0 Hz, CH_3); δ_C ($CDCl_3$) 177.2, 163.8, 158.9, 136.6, 128.4, 128.1, 127.9, 66.9, 64.6, 41.8, 9.5; ν_{max} 3378, 3286, 3033, 2980, 2944, 2872, 2833, 2789, 1708, 1649, 1619, 1528, 1498, 1439, 1263, 1082 cm^{-1}; MS (ESI) m/z 293.2 (100%, $[M + H]^+$); HRMS (ESI) found 293.1614, m/z $C_{14}H_{21}N_4O_3^+$ $[M + H]^+$ requires 293.1614.

(*S*)-*N*-Cbz-*N*′-carbamimidoyl-2-(dimethylamino)-3-phenylpropanamide 43b: method A. *N*-Dimethyl-L-phenylalanine **42b** (800.2 mg, 4.14 mmol, 1.0 equiv.); DMF (15 mL); CDI (1.43 g, 8.28 mmol, 2.0 equiv.); 24 h; *N*-Cbz-guanidine (800.0 mg, 4.14 mmol, 1.0 equiv.); 6 d. Extraction and column chromatography (33–42% EA in PE) gave **43b** (1.20 g, 3.26 mmol) as a white solid in 79% yield. R_f 0.1 (50% EA in PE); $[\alpha]_D^{23}$ +30.0 (CH_2Cl_2, $c = 3.0$); mp 141–143 °C, δ_H ($CDCl_3$) 7.99–10.49 (3H, br s, 3× NH) 7.11–7.32 (10H, m, 2× Ph) 5.05 (2H, s, CH_2), 3.36 (1H, dd, J 5.8, 7.4 Hz, CH), 3.04 (1H, dd, J 7.4, 14.0 Hz, CH), 2.85 (1H, dd, J 5.8, 14.0 Hz, CH), 2.23 (6H, s, 2× CH_3); δ_C ($CDCl_3$) 175.8, 163.6, 158.8, 138.9, 136.6, 129.1, 128.7, 128.5, 128.2,

128.0, 126.6, 71.3, 67.1, 42.0, 31.3; ν_{max} 3381, 3284, 3063, 3030, 2929, 2789, 1704, 1650, 1621, 1530, 1496, 1453, 1268, 1165 cm^{-1}; MS (ESI) *m/z* 385.2 (100%, $[M + H_2O–H]^+$), 369.2 (43%, $[M + H]^+$); HRMS (ESI) *m/z* found 369.1926, $C_{20}H_{25}N_4O_3^+$ $[M + H]^+$ requires 369.1921.

(*S*)-*N*-Boc-*N′*-carbamimidoyl-2-(dimethylamino)propanamide 44a: method A. *N*-Methyl-L-alanine **42a** (883.1 mg, 7.54 mmol, 1.2 equiv.) DMF (20 mL); CDI (1.73 g, 10.68 mmol, 1.7 equiv.) 6 h; *N*-Boc-guanidine (1.0 g, 6.28 mmol, 1.0 equiv.); 4 d. Extraction and column chromatography (0–0.5% ME in CF) gave **44a** (0.65 g, 2.52 mmol) as a white solid in 40% yield. R_f 0.14 (DE); $[\alpha]_D^{18}$ +27.8 (CH_2Cl_2, $c = 1.05$); mp 119–120 °C; δ_H ($CDCl_3$) 8.96 (3H, br s, 3× NH), 3.12 (1H, q, *J* 6.9 Hz, CH), 2.22 (6H, s, CH_3), 1.49 (3H, s, 3× Me), 1.20 (3H, d, *J* 7.0 Hz, CH_3); δ_C ($CDCl_3$) 177.3, 158.6, 79.5, 64.9, 41.9, 28.3, 9.8; ν_{max} 3380, 3129, 2972, 2938, 2871, 2832, 2791, 1712, 1653, 1564, 1478, 1136, 1049 cm^{-1}; MS (ESI) *m/z* 275.2 (100%, $[M + H_2O–H]^+$), 259.3 (43%, $[M + H]^+$); HRMS (ESI) *m/z* found 259.1768, $C_{11}H_{23}N_4O_3^+$ ($[M + H]^+$) requires 259.1765.

(*S*)-*N*-Boc-*N′*-carbamimidoyl-2-(dimethylamino)-3-phenylpropanamide 44b: method A. *N*-Methyl-L-phenylalanine **42b** (1.00 g, 5.17 mmol, 1.0 equiv.); DMF (20 mL); CDI (1.30 g, 7.76 mmol, 1.55 equiv.); 24 h; *N*-Boc-guanidine (823.8 mg, 5.17 mmol, 1.0 equiv.); 13 d. Extraction and column chromatography (17–28% EA in PE) gave **44b** (1.5 g, 4.49 mmol) as a white solid in 87% yield. R_f 0.16 (50% EA/PE); $[\alpha]_D^{18}$ +37.0 (CH_2Cl_2, $c = 1.9$); mp 101–103 °C; δ_H ($CDCl_3$) 8.95 (3H, br s, NH), 7.30–7.15 (5H, m, CH), 3.42–3.35 (1H, m, CH), 3.08 (1H, dd, *J* 14.0, 7.4 Hz, CH_2), 2.88 (1H, d, *J* 5.9 Hz, CH_2), 2.27 (6H, s, CH_3), 1.47 (9H, s, CH_3); δ_C ($CDCl_3$) 176.0, 162.9, 158.4, 138.9, 129.1, 128.6, 126.5, 79.5, 71.4, 42.0, 31.5, 28.2; ν_{max} 3386, 3285, 2975, 2935, 2832, 2789, 1702, 1654, 1620, 1561, 1530, 1495, 1293 cm^{-1}; MS (ESI) 351.2 (100%, $[M + H_2O–H]^+$), 335.2 (100%, $[M + H]^+$); HRMS (ESI) *m/z* found 335.2082, $C_{17}H_{27}N_4O_3^+$ ($[M + H]^+$), requires 335.2078.

(*S*)-2-(Dimethylamino)-3-phenyl-*N*-(*N′*-phenylcarbamimidoyl) propanamide 45b method B. *N,N*-Dimethyl-L-phenylalanine **42b** (1.0 g, 5.17 mmol, 1.0 equiv.); DMF (15 mL), CDI (1.82 g, 11.21 mmol, 2.6 equiv.); 24 h; NaH (60%, 155.2 mg, 3.88 mmol, 1.0 equiv.); DMF (15 mL); phenylguanidinium carbonate (850.4 mg, 4.31 mmol, 1.0 equiv.); 4 d. Extraction and column chromatography (50–100% EA in PE) gave **45b** (0.61 g, 1.97 mmol) as a pale yellow gum in 46% yield. R_f 0.1 (EA); $[\alpha]_D^{19}$ +49.7 (CH_2Cl_2, $c = 2.15$); δ_H ($CDCl_3$) 7.09–7.51 (11H, m, NH, NH_2, Ph, 3× CH), 7.02 (2H, br d, *J* 8 Hz, 2× CH), 3.50 (1H, dd, *J* 6.2, 7.1 Hz, CH), 3.22 (1H, dd, *J* 7.1, 14.2 Hz, CH), 2.95 (1H, dd, *J* 6.2, 14.1, Hz, CH), 2.38 (6H, s, 2× CH_3); δ_C ($CDCl_3$) 175.3, 149.6, 144.6, 139.4, 129.8, 129.2, 128.7, 126.5, 124.2, 123.3, 71.5, 42.1, 31.8; ν_{max} 3309, 3060, 3027, 2940, 2866, 2830, 2785, 1655, 1589, 1561, 1509, 1493, 1077 cm^{-1}; MS (ESI −ve) *m/z* 345.2 (52%, $[M + Cl]^-$), 309.2 (77%, $[M - H]^-$), 264 (100%); HRMS (ESI −ve) *m/z* found 309.1720, $C_{18}H_{21}N_4O^-$ ($[M - H]^-$) requires 309.1721.

(*S*)-*N*-(1*H*-Benzo[*d*]imidazol-2-yl)-2-(dimethylamino)propanamide 46a: method A. *N,N*-Dimethyl-L-alanine **42a** (500.0 mg, 3.76 mmol, 1.0 equiv.); DMF (7 mL); CDI (1.52 g, 9.39 mmol, 2.5 equiv.); 24 h; 2-aminobenzimidazole (659.8 mg, 5.63 mmol, 1.5 equiv.) 24 h. Extraction and column chromatography (60–90% EA in PE) gave **46a** (800.0 mg, 3.44 mmol) as a white solid in 92% yield. R_f 0.10 (EA); $[\alpha]_D^{20}$ +24.3 (CH_3Cl, $c = 1.07$); mp 208–210 °C; δ_H (D_6-DMSO) 12.08 (1H, br s, NH), 11.20 (1H, br s, NH), 7.37–7.50 (2H, m, 2× CH), 7.07–7.09 (2H, m, 2 × CH), 3.32 (1H, q, *J* 6.8 Hz, CH), 2.28 (6H, s, 2× CH_3), 1.20 (3H, d, *J* 6.8 Hz, CH_3); δ_C ($CDCl_3$) 172.5, 146.2, 140.5 (HMBC), 134.4 (HMBC), 121.0, 62.2, 41.2, 12.4; ν_{max} 3335, 3100, 2978, 2942, 2870, 2826, 2782, 1683, 1562, 1520, 1455, 1222 cm^{-1}; MS (ESI) *m/z* 233.1 (100%, $[M + H]^+$), 161.1 (44%); HRMS (ESI) *m/z* found 233.1404, $C_{12}H_{17}N_4O^+$ ($[M + H]^+$) requires 233.1402.

(*S*)-*N*-(1*H*-Benzo[*d*]imidazol-2-yl)-2-(dimethylamino)-3-phenylpropanamide 46b: method A. *N,N*-Dimethyl-L-phenylalanine **42b** (800.0 mg, 4.14 mmol, 1.0 equiv.); DMF (15 mL); CDI (1.64 g, 10.10 mmol, 2.44 equiv.); 24 h; 2-aminobenzimidazole (551.2 mg, 4.14 mmol, 1.0 equiv.); 7 d. Brine (100 mL) was added, extraction and column chromatography (0–30% EA in DE) gave **46b** (540.0 mg, 1.75 mmol) as a white solid in 42% yield. R_f 0.06 (DE); $[\alpha]_D^{20}$ +33.5 (MeOH, $c = 2.6$); mp 133–136 °C; δ_H ($CDCl_3$) 10.32 (2H, br s, 2× NH), 7.44–7.46 (2H, m, 2× CH), 7.13–7.25 (7H, m, Ph, 2× CH), 3.57 (1H, dd, *J* 5.7, 7.8 Hz, CH), 3.21 (1H, dd, *J* 7.8, 13.9 Hz, CH), 2.97 (1H, dd, *J* 5.7, 13.9 Hz, CH), 2.35 (6H, s, 2× CH_3); δ_C ($CDCl_3$) 172.9, 146.7, 141.0 (HMBC), 138.7, 129.0, 128.5, 126.5, 122.3, 70.6, 42.0, 32.5; ν_{max} 3372, 3027, 2885, 2785, 1682, 1630, 1561, 1519, 1455, 1272 cm^{-1}; MS (ESI) *m/z* 309.2 (100%, $[M + H]^+$); HRMS (ESI) *m/z* found 309.1712, $C_{18}H_{21}N_4O^+$ ($[M + H]^+$) requires 309.1710.

(*S*)-*N*-(Amino((*S*)-2-(dimethylamino)-3-phenylpropanamido) methylene)-2-(dimethylamino)-3-phenylpropanamide 47b method C. *N,N*-Dimethyl-L-phenylalanine **42b** (1.0 g, 5.17 mmol, 1.0 equiv.); DMF (10 mL); CDI (1.43 g, 8.80 mmol, 1.7 equiv.); 24 h; guanidinium hydrochloride (247.2 mg, 2.59 mmol, 0.5 equiv.); DMF (10 mL); NaH (60%, 124.1 mg, 9.54 mmol, 3.1 equiv.), 7 d. Extraction and column chromatography (90–100% DE in PE; 0–100% EA in DE with Et_3N (3 drop per litre)) gave **47b** (820.0 mg, 2.00 mmol) as an off-white wax in 77% yield. R_f 0.15 (100% EA + 3 drops NH_4OH); $[\alpha]_D^{21}$ +61.9 (CH_2Cl_2, $c = 1.38$); δ_H ($CDCl_3$) 8.06–10.04 (2H, s, 2× NH), 7.20–7.24 (10H, m, 2× Ph), 3.39 (2H, dd, *J* 5.3, 8.5 Hz, 2× CH), 3.12 (2H, dd, *J* 8.6, 13.6 Hz, 2× CH), 2.98 (2H, dd, *J* 5.3, 13.6 Hz, 2× CH), 2.41 (12H, s, 4× CH_3); δ_C ($CDCl_3$) 178.8, 157.9, 139.2, 129.3, 128.5, 126.4, 73.1, 42.4, 33.1; ν_{max} 3365, 3062, 2965, 2935, 2829, 2785, 1703, 1633, 1602, 1450, 1453, 1078 cm^{-1}; MS (ESI) *m/z* 410.3 (100%, $[M + H]^+$); HRMS (ESI) *m/z* found 410.2543, $C_{23}H_{31}N_5O_2^+$ ($[M + H]^+$) requires 410.2551.

General method for the reaction of 2-hydroxy-1,4-naphthoquinone 93 with β-nitrostyrene 52

2-Hydroxy-1,4-napthoquinone **1** (100 mg, 0.574 mmol) and the required catalyst (0.04–0.1 equiv.) were dissolved in the required solvent and cooled to the required temperature (−20 to 0 °C, see Table 1). β-Nitrostyrene **2** (128.5 mg, 0.861 mmol, 1.5 equiv.) was then added and the mixture stirred for the required time and temperature. Reaction progress was determined by sampling and H NMR analysis. On completion the solvent was evaporated to give a deep red residue which was purified by column chromatography eluting firstly with 2–4% EA in petrol to remove excess **2** then followed with DCM to give the product **5**

as a yellow solid. Illustrative example from catalyst **25a**; 56% ee, $[\alpha]_D^{25}$ −16.0 (acetone, c = 1.46); lit. $[\alpha]_D^{17}$ −44.8 (acetone, c = 1.0),[14] lit. $[\alpha]_D^{25}$ −34.0 (acetone, c = 1.46).[15] Enantiomeric excess were determined either on a Chiralcel AS-H (250 × 4.6 mm, mobile phase 96% hexane, 4% isopropanol, 0.1% TFA, 1.5 mL min^{-1} at 40 °C, detecting at 254 nm; *R* enantiomer 23.5 min, *S* enantiomer 26.2 min) or a Phenomenex Lux Amylose-1 (250 × 4.6 mm, mobile phase 70% hexane, 30% isopropanol, 0.5 mL min^{-1} at 40 °C, detecting at 254 nm; *R* enantiomer 13.2 min, *S* enantiomer 14.3 min).

X-ray diffraction studies

Catalysts **25a**, **34c**, **40b** and **40d**, were collected on an Rigaku AFC12 goniometer equipped with an enhanced sensitivity (HG) Saturn724+ detector mounted at the window of an FR-E+ Super Bright molybdenum rotating anode generator with HF Varimax optics (100 μm focus). The cell determination and data collection were carried out using the CrystalClear-SM Expert package (Rigaku, 2012) data reduction cell refinement and absorption correction were carried out using CrysAlisPro software (Rigaku OD, 2015).[16]

Catalysts **30**, **34a**, **39**, **41b**, **41c**-*crystal 1*, **43a** and **44b** were collected on an Rigaku AFC11 goniometer equipped with an Hypix 6000 detector mounted at the window of an 007HF copper rotating anode generator with HF Varimax optics (150 μm focus). Cell determination data collection, data reduction cell refinement and absorption correction were carried out using CrysAlisPro software (Rigaku OD, 2015).[16]

Catalysts **26a**, **26c**, **26d**, **27a**, **29**, **31**, **34b**, **38b**, **41c**-*crystal 2* and **43b** were collected at the synchrotron Diamond Light Source (beamtime I19)[17] using a Dectris Pilatus 2M detector (CCDC numbers: 1952629–1952649). Data collection was carried out using the beamline control software, data reduction cell refinement and absorption correction were carried out using XIA2.[18] All structures were initially solved and refined using SHELXT and SHELXL-2014 [19] within OLEX-2.[20]

Conflicts of interest

There are no conflicts to declare.

Acknowledgements

We thank the EPSRC (DE, EP/J01821X/1), the ERASMUS and SOCRATES schemes (FFJDK), BEACON (ERDF; DE, PJM), the Iraqi government (ZSSA-T) and the government of Saudi Arabia (YTHM) for funding and support. This work was carried out with the support of the Diamond Light Source, instrument I19 (proposal MT15762). We also thank the EPSRC National Crystallography Service at the University of Southampton and the National Mass Spectrometry Facility at Swansea for their excellent work.

References

1 M. T. Allingham, E. L. Bennett, D. H. Davies, P. M. Harper, A. Howard-Jones, Y. T. H. Mehdar, P. J. Murphy, D. A. Thomas, P. W. R. Caulkett, D. Potter, C. M. Lam and A. C. O'Donoghue, *Tetrahedron*, 2016, **72**, 496–503.
2 S. Bhowmick, A. Mondal, A. Ghosh and K. C. Bhowmick, *Tetrahedron: Asymmetry*, 2015, **26**, 1215–1244.
3 P. J. Murphy, M. St. Allingham and A. J. L. Howard-Jones, *Tetrahedron*, 2003, **44**, 8677–8680.
4 Z. Yu, X. Liu, L. Zhou, L. Lin and X. Feng, *Angew. Chem., Int. Ed.*, 2009, **48**, 5195–5198.
5 M. Terada, T. Ikehara and H. Ube, *J. Am. Chem. Soc.*, 2007, **129**, 14112–14113.
6 D. Almasi, D. A. Alsono, E. Gomez-Bengoa and C. Najera, *J. Org. Chem.*, 2009, **74**, 6163–6168.
7 E. Gomez-Torres, D. A. Alonso, E. Gomez-Bengoa and C. Najera, *Org. Lett.*, 2011, **13**, 6106–6109.
8 T. E. Shubina, M. Freund, S. Schenker, T. Clark and S. B. Tsogoeva, *Beilstein J. Org. Chem.*, 2012, **8**, 1485–1498.
9 G. Tang, Ü. Gün and H. Altenbach, *Tetrahedron*, 2012, **68**, 10230–10235.
10 S. Bhowmick, S. S. Kunte and K. C. Bhowmick, *RSC Adv.*, 2014, **4**, 24311–24315.
11 A. D. G. Yamagata and D. J. Dixon, *Org. Lett.*, 2017, **19**, 1894–1897.
12 G. Moore, Novel phosphonium salts and bifunctional organocatalysts in asymmetric synthesis, PhD thesis, University of Nottingham, 2013.
13 Z. Han, R. Wang, Y. Zhou and L. Liu, *Eur. J. Org. Chem.*, 2005, 934–938.
14 S. B. Woo and D. Y. Kim, *Beilstein J. Org. Chem.*, 2012, **8**, 699–704.
15 W. Yang and D. Du, *Adv. Synth. Catal.*, 2011, **353**, 1241–1246.
16 O. D. Rigaku, *CrysAlis PRO*, Rigaku Oxford Diffraction Ltd, Yarnton, England, 2015.
17 (*a*) D. R. Allan, H. Nowell, S. A. Barnett, M. R. Warren, A. Wilcox, J. Christensen, L. K. Saunders, A. Peach, M. T. Hooper, L. Zaja, S. Patel, L. Cahill, R. Marshall, S. Trimnell, A. J. Foster, T. Bates, S. Lay, M. A. Williams, P. V. Hathaway, G. Winter, M. Gerstel and R. W. Wooley, *Crystals*, 2017, **7**(11), 336; (*b*) H. Nowell, S. A. Barnett, K. E. Christensen, S. J. Teat and D. R. Allan, *J. Synchrotron Radiat.*, 2012, **19**, 435–441.
18 G. Winter, *J. Appl. Crystallogr.*, 2010, **43**, 186–190.
19 G. M. Sheldrick, *Acta Crystallogr., Sect. C: Struct. Chem.*, 2015, **71**, 3–8.
20 O. V. Dolomanov, L. J. Bourhis, R. J. Gildea, J. A. K. Howard and H. J. Puschmann, *Appl. Crystallogr.*, 2009, **42**, 339–341.

